Phage infection and sub-lethal antibiotic exposure mediate *Enterococcus faecalis* type VII secretion system dependent inhibition of bystander bacteria

Anushila Chatterjee[a]*, Julia L. E. Willett[b]*, Gary M. Dunny[b], Breck A. Duerkop[a,#]

[a]Department of Immunology and Microbiology, University of Colorado School of Medicine, Aurora, CO, USA, 80045. [b]Department of Microbiology and Immunology, University of Minnesota Medical School, Minneapolis, MN, USA, 55455.

[#]Correspondence: Breck A. Duerkop breck.duerkop@cuanschutz.edu

*A.C. and J.L.E.W. contributed equally to this work.

Running title: Phage and antibiotic induced T7SS promotes antibacterial antagonism

Key words: bacteriophages, *Enterococcus*, antibiotic resistance, phage–bacteria interactions, bacterial secretion systems, type VII secretion, contact-dependent antagonism

Abstract

Bacteriophages (phages) are being considered as alternative therapeutics for the treatment of multidrug resistant bacterial infections. Considering phages have narrow host-ranges, it is generally accepted that therapeutic phages will have a marginal impact on non-target bacteria. We have discovered that lytic phage infection induces transcription of type VIIb secretion system (T7SS) genes in the pathobiont *Enterococcus faecalis*. Membrane damage during phage infection induces T7SS gene expression resulting in cell contact dependent antagonism of different Gram positive bystander bacteria. Deletion of *essB*, a T7SS structural component, abrogates phage-mediated killing of bystanders. A predicted immunity gene confers protection against T7SS mediated inhibition, and disruption of its upstream LXG toxin gene rescues growth of *E. faecalis* and *Staphylococcus aureus* bystanders. Phage induction of T7SS gene expression and bystander inhibition requires IreK, a serine/threonine kinase, and OG1RF_11099, a predicted GntR-family transcription factor. Additionally, sub-lethal doses of membrane targeting and DNA damaging antibiotics activated T7SS expression independent of phage infection, triggering T7SS antibacterial activity against bystander bacteria. Our findings highlight how phage infection and antibiotic exposure of a target bacterium can affect non-target bystander bacteria and implies that therapies beyond antibiotics, such as phage therapy, could impose collateral damage to polymicrobial communities.

Introduction

Enterococci constitute a minor component of the healthy human microbiota [1]. Enterococci, including *Enterococcus faecalis*, are also nosocomial pathogens that cause a variety of diseases, including sepsis, endocarditis, surgical-site, urinary tract and mixed bacterial infections [2, 3]. Over recent decades, enterococci have acquired extensive antibiotic resistance traits, including resistance to “last-resort” antibiotics such as vancomycin, daptomycin, and linezolid [4-8]. Following antibiotic therapy, multi-drug resistant (MDR) enterococci can outgrow to become a dominant member of the intestinal microbiota, resulting in intestinal barrier invasion and blood stream infection [7, 9]. The ongoing evolution of MDR enterococci in healthcare settings [4-6, 10, 11] and their ability to transmit antibiotic resistance among diverse bacteria [9, 12-15], emphasize the immediate need for novel therapeutic approaches to control enterococcal infections.

Viruses that infect and kill bacteria (bacteriophages or phages) are receiving attention for their use as antibacterial agents [16]. Recent studies have demonstrated the efficacy of anti-enterococcal phages in murine models of bacteremia [17-19] and the administration of phages to reduce *E. faecalis* burden in the intestine gives rise to phage resistant isolates that are sensitized to antibiotics [20]. Considering phages are highly specific for their target bacterium, coupled with the self-limiting nature of their host-dependent replication, this suggests that unlike antibiotics which have broad off-target antimicrobial activity, phages should have nominal impact on bacteria outside of their intended target strain [21-23]. However, our understanding of how phages interact with bacteria and the bacterial response to phage infection is limited.

While studying the transcriptional response of phage infected *E. faecalis* cells, we discovered that phage infection induces the expression of genes involved in the biosynthesis of a type VIIb secretion system (T7SS) [24]. Firmicutes, including the enterococci, harbor diverse T7SS genes encoding transmembrane and cytoplasmic proteins involved in the secretion of protein substrates [25], and T7SSs promote antagonism of non-kin bacterial cells through

contact-dependent secretion of antibacterial effectors and/or toxins [26, 27]. The antibacterial activity of T7SSs from staphylococci and streptococci are well characterized [25] but T7SS-mediated antibacterial antagonism has not been described for enterococci. The environmental cues and regulatory pathways that govern T7SS expression and activity are poorly understood, although recent studies indicate that exposure to serum and membrane stresses triggered by pulmonary surfactants, fatty acids and phage infection stimulate T7SS gene expression [24, 28-31]. This motivated us to determine if phage induced T7SS gene expression in *E. faecalis* results in the inhibition of non-kin bacterial cells that are not phage targets (bystanders). We discovered that phage infected *E. faecalis* produces potent T7SS antibacterial activity against bystander bacteria. Expression of a T7SS antitoxin (immunity factor) gene in bystander cells and mutation of the LXG domain containing gene located immediately upstream of this immunity factor confer protection against phage mediated T7SS inhibition. We also investigated the potential impact of antimicrobials directed against bacterial physiological processes that are also targeted by phages, including cell wall, cell membrane and DNA damaging agents, on enterococcal T7SS. Sub-lethal challenge with specific antibiotics enhances T7SS gene expression resulting in T7SS dependent interspecies antagonism. Additionally, we discovered that membrane stress during phage infection induces transcription of T7SS genes via a non-canonical IreK signaling pathway. To our knowledge, the enterococcal T7SS is the first example of secretion system induction during phage infection. These data shed light on how phage infection of a cognate bacterial host can influence polymicrobial interactions and raises the possibility that phages may impose unintended compositional shifts among bystander bacteria in the microbiota during phage therapy.

Results

Phage mediated induction of *E. faecalis* T7SS leads to interspecies antagonism.

A hallmark feature of phage therapy is that phages often have a narrow host range, hence they do not influence the growth of non-susceptible bacteria occupying the same niche [22]. We discovered that infection of *E. faecalis* OG1RF by phage VPE25 induces the expression of T7SS genes [24]. The *E. faecalis* OG1RF T7SS locus is absent in the commonly studied vancomycin-resistant strain V583, despite conservation of flanking genes (Fig. 1A) [32, 33]. The OG1RF T7SS is found downstream of conserved tRNA-Tyr and tRNA-Gln genes, which could facilitate recombination or integration of new DNA [34], but no known recombination or integration sites were identified on the 3' end of this locus. Homologs of the *E. faecalis* T7SS gene *esxA* are found throughout three of the four *Enterococcus* species groups [35], including *Enterococcus faecium*, suggesting a wide distribution of T7SS loci in enterococci (Fig. S1). In addition to EsxA, OG1RF encodes the core T7SS structural components EsaA, EssB, and EssC, which are predicted to localize to the membrane, and EsaB, a small predicted cytoplasmic protein (Fig. 1A) [36]. OG1RF_11102 encodes an additional putative membrane protein, although it does not share sequence homology with staphylococcal or streptococcal EssA. We were unable to identify an EssA homolog in OG1RF using sequence-based homology searches, suggesting that the enterococcal T7SS machinery may differ from previously described T7SS found in other Gram-positive bacteria. *In silico* analyses predict that the *E. faecalis* T7SS locus encodes multiple WXG100 family effectors and LXG family polymorphic toxins [27, 37]. We hypothesized that induction of T7SS genes during phage infection and consequently the heightened production of T7SS substrates would indirectly influence the growth of non-kin phage-resistant bacterial cells.

To investigate if T7SS factors produced during phage infection of *E. faecalis* OG1RF interferes with the growth of phage-resistant bystander bacteria, we generated a strain with an in-frame deletion in the T7SS gene *essB*, encoding a transmembrane protein involved in the transport of T7SS substrates [38]. We chose to inactivate *essB* as opposed to the more commonly investigated secretion promoting ATPase *essC* [27, 38], because *E. faecalis* OG1RF

harbours two *essC* genes in its T7SS locus that may have functional redundancy (Fig. 1A). The *essB* mutant is equally susceptible to phage VPE25 infection compared to wild type *E. faecalis* OG1RF (Fig. S2A). We performed co-culture experiments where phage susceptible wild type *E. faecalis* OG1RF or Δ*essB* were mixed with a phage resistant bystander, a strain of *E. faecalis* V583 deficient in the production of the VPE25 receptor (Δpip_{V583}) [39], at a ratio of 1:1 in the absence and presence of phage VPE25 (multiplicity of infection [MOI] = 0.01) (Fig. 1B). VPE25 infected *E. faecalis* OG1RF and the Δ*essB* mutant with similar efficiency and caused a 1000-fold reduction in the viable cell count over a period of 24 hours (Fig. S2B). Since sequence-based homology searches did not retrieve any homologs of potential antitoxins from the *E. faecalis* OG1RF T7SS locus in *E. faecalis* V583 genome, this strain likely lacks immunity to toxins encoded in this locus. The viability of *E. faecalis* Δpip_{V583}, was reduced nearly 100-fold when co-cultured with *E. faecalis* OG1RF in the presence of phage VPE25 (Fig. 1C, S2C). However, growth inhibition of *E. faecalis* Δpip_{V583} was abrogated during co-culture with phage infected *E. faecalis* Δ*essB* and phage induced T7SS antagonism of *E. faecalis* Δ*essB* could be restored by complementation (Fig. 1C, S2C), indicating that inhibition of phage resistant *E. faecalis* Δpip_{V583} by OG1RF is T7SS dependent.

T7SS encoded antibacterial toxins secreted by Gram positive bacteria influence intra- and interspecies antagonism [26, 27]. While a nuclease and a membrane depolarizing toxin produced by *Staphylococcus aureus* target closely related *S. aureus* strains [26, 40], *Streptococcus intermedius* exhibits T7SS dependent antagonism against a wide-array of Gram positive bacteria [27]. To determine the target range of *E. faecalis* OG1RF T7SS antibacterial activity, we measured the viability of a panel of VPE25 insensitive Gram positive and Gram negative bacteria in our co-culture assay (Fig. 1B). Growth inhibition of the distantly related bacterial species *E. faecium* and Gram positive bacteria of diverse genera, including *S. aureus* and *Listeria monocytogenes*, occurred following co-culture with phage infected wild type *E. faecalis* OG1RF but not the Δ*essB* mutant (Fig. 1D). Fitness of *Lactococcus lactis,* a lactic acid

bacterium like *E. faecalis*, was modestly reduced during co-culture with phage infected *E. faecalis* OG1RF, although these data were not statistically significant. In contrast, Gram positive pathogenic and commensal streptococci were unaffected (Fig. 1D). Similarly, phage induced T7SS activity did not inhibit any Gram negative bacteria tested (Fig. 1D). Collectively, these results show that phage predation of *E. faecalis* promotes T7SS inhibition of select bystander bacteria.

Molecular basis of *E. faecalis* phage–triggered T7SS antagonism

Our data demonstrate that induction of *E. faecalis* OG1RF T7SS genes during phage infection hinder the growth of select non-kin bacterial species. Antibacterial toxins deployed by Gram negative bacteria via type V and VI secretion and Gram positive T7SS require physical contact between cells to achieve antagonism [26, 27, 41, 42]. Therefore, we investigated if growth inhibition of bystander bacteria is contingent upon direct interaction with phage infected *E. faecalis* using a trans-well assay [27]. We added unfiltered supernatants from wild type *E. faecalis* OG1RF and Δ*essB* mutant cultures grown for 24 hrs in the presence and absence of phage VPE25 (MOI = 0.01) to the top of a trans well and deposited phage resistant *E. faecalis* Δpip_{V583} in the bottom of the trans well. The 0.4 µm membrane filter that separates the two wells is permeable to proteins and solutes but prevents bacterial translocation. Supernatant from phage infected wild type *E. faecalis* OG1RF did not inhibit *E. faecalis* Δpip_{V583} (Fig. S3A) indicating that T7SS mediated growth interference relies on cell to cell contact. To exclude the possibility that T7SS substrates might adhere to the 0.4 µm membrane filter in the trans-well assay, we administered both filtered and unfiltered culture supernatants directly to *E. faecalis* Δpip_{V583} cells ($5x10^5$ CFU/well) at a ratio of 1:10 (supernatant to bystander cells) and monitored growth over a period of 10 hours. Growth kinetics of *E. faecalis* Δpip_{V583} remained similar irrespective of the presence or absence of conditioned supernatant from wild type *E. faecalis*

OG1RF or Δ*essB* mutant cultures (Fig. S3B – S3C), further supporting the requirement of contact-dependent engagement of phage mediated T7SS inhibition.

We discovered that *E. faecalis* OG1RF inhibits proliferation of non-kin bacterial cells through increased expression of T7SS genes in response to phage infection, but the toxic effectors were unknown. LXG domain containing toxins are widespread in bacteria with a diverse range of predicted antibacterial activities [43, 44]. The OG1RF T7SS locus encodes two LXG-domain proteins, OG1RF_11109 and OG1RF_11121 (Fig. 2A). Both LXG domains were found using Pfam, but we were unable to identify predicted function or activity for either protein using sequence homology searches or structural modeling.

Bacterial polymorphic toxin systems can encode additional toxin fragments and cognate immunity genes, known as “orphan” toxin/immunity modules, downstream of full-length secreted effectors [45, 46]. Orphan toxins lack the N-terminal domains required for secretion or delivery, although they can encode small regions of homology that could facilitate recombination with full-length toxin genes [47]. Therefore, we sought to identify putative orphan toxins in OG1RF. We aligned the nucleotide sequences of OG1RF_11109 and OG1RF_11121 with downstream genes in the T7SS locus and looked for regions of similarity that might signify orphan toxins. Although the 3’ ends of OG1RF_11111 and OG1RF_11113 did not have homology to either OG1RF_11109 or OG1RF_11121, the 5’ ends of OG1RF_11111 and OG1RF_11113 had >75% nucleotide homology to a portion of OG1RF_11109 (Fig. 2A, regions of homology indicated by gray shading). Similarly, OG1RF_11123 had sequence homology to OG1RF_11121 (Fig. 2A). We searched Pfam and ExPasy for annotated domains but were unable to identify any in OG1RF_11111, OG1RF_11113, or OG1RF_11123. However, structural modeling with Phyre2 [48] revealed that a portion of OG1RF_11123 has predicted structural homology to the channel-forming domain of colicin 1a [49] (Fig. S4D).

Orphan toxins encoded by a secretion system in a given strain can often be found as full-length toxins in other bacteria [45, 46]. Therefore, we used the sequences of OG1RF_11111,

OG1RF_11113, and OG1RF_11123 as input for NCBI Protein BLAST to determine whether the orphan toxins we identified in *E. faecalis* OG1RF were found in other T7SS loci. We identified homologs to these orphan toxins in other *E. faecalis* strains as well as *Listeria sp*. (Fig. S4A-C, gray shading indicates regions of homology). These homologs were longer than the *E. faecalis* OG1RF genes and encoded N-terminal LXG domains, suggesting that in *Listeria* and other *E. faecalis* strains, homologs to OG1RF_11111, 11113, and 11123 are full-length toxins that could be secreted by the T7SS.

Interestingly, we identified an additional LXG gene product, OG1RF_12414, in a distal locus that is again notably absent from *E. faecalis* V583 (Fig. S5A and S5B). OG1RF_12414 has predicted structural homology to Tne2, a T6SS effector with NADase activity from *Pseudomonas protegens* (Fig. S5C) [50]. Additionally, we identified numerous C-terminal domains in LXG proteins distributed throughout the enterococci (Fig. S6). These include EndoU and Ntox44 nuclease domains [43, 51, 52], which have been characterized in effectors produced by other polymorphic toxin systems.

Polymorphic toxins are genetically linked to cognate immunity proteins that neutralize antagonistic activity and prevent self-intoxication [43, 52, 53]. Each of the five putative toxins in the OG1RF T7SS locus is encoded directly upstream of a small protein that could function in immunity. Whitney *et al*. demonstrated that the cytoplasmic antagonistic activity of *S. intermedius* LXG toxins TelA and TelB in *Escherichia coli* can be rescued by co-expression of cognate immunity factors [27]. Therefore, we examined if OG1RF_11110, 11112, 11122, or 12413 confer immunity to *E. faecalis* Δpip_{V583} during phage infection of *E. faecalis* OG1RF. Constitutive expression of OG1RF_11122, and not OG1RF_11110, 11112, or 12413, partially neutralized phage induced T7SS antagonism (Fig. 2B), confirming an essential role for the OG1RF_11122 gene product in immunity, and suggesting that OG1RF_11121 is at least partly responsible for T7SS mediated intra-species antagonism. However, further investigation is

needed to confirm whether the candidate immunity factors, OG1RF_11110, 11112 or 12413, are stably expressed under these experimental conditions.

To determine the contribution of OG1RF_11121 on intra- and interbacterial antagonism during phage infection, we measured the viability of phage resistant *E. faecalis* Δpip_{V583} and *S. aureus* in co-culture with an *E. faecalis* OG1RF variant carrying a transposon insertion in OG1RF_11121 (OG1RF_11121-Tn). OG1RF_11121-Tn is equally susceptible to phage VPE25 infection compared to wild type *E. faecalis* OG1RF (Fig. S2A). Similar to the Δ*essB* (pCIEtm) strain carrying empty pCIEtm plasmid, phage infected OG1RF_11121-Tn (pCIEtm) did not inhibit the growth of the bystander bacteria (Fig. 2C – 2D). We were unable to clone OG1RF_11121 by itself into the inducible plasmid pCIEtm, suggesting leaky expression of OG1RF_11121 is toxic. Therefore, to complement *E. faecalis* OG1RF_11121-Tn we cloned both the OG1RF_11121 toxin and OG1RF_11122 antitoxin pair under the cCF10-inducible promoter in pCIEtm. Expression of both of these genes in the transposon mutant restored its ability antagonize T7SS susceptible bystanders (Fig. 2C – D). These data strongly suggest that the OG1RF_11121 encoded LXG toxin drives *E. faecalis* T7SS mediated antagonism of bystanders following phage infection.

Sub-lethal antibiotic stress promotes T7SS dependent antagonism

Considering two genetically distinct phages trigger the induction of T7SS genes in *E. faecalis* [24], we reasoned that T7SS induction could be a result of phage mediated cellular damage and not specifically directed by a phage encoded protein. Antibiotics elicit a range of damage induced stress responses in bacteria [54-56]; therefore, independent of phage infection we investigated the effects of subinhibitory concentrations of antibiotics on T7SS expression in *E. faecalis*.

To investigate the influence of sublethal antibiotic concentrations on *E. faecalis* OG1RF T7SS transcription, we determined the minimum inhibitory concentrations (MIC) of ampicillin,

vancomycin, and daptomycin (Fig.S7A – S7C) and monitored T7SS gene expression in *E. faecalis* OG1RF cells treated with a sub-lethal dose of antibiotic (50% of the MIC). We found that bacterial T7SS genes were significantly upregulated in the presence of the cell membrane targeting antibiotic, daptomycin, relative to the untreated control (Fig. 3A). In contrast, the cell wall biosynthesis inhibitors ampicillin and vancomycin either did not induce or had a minor impact on T7SS mRNA levels, respectively (Fig.3A). Additionally, induction of T7SS transcription occurred when bacteria were challenged with sub-inhibitory concentrations of the DNA targeting antibiotics ciprofloxacin and mitomycin C (Fig.3B, Fig. S7D – S7E).

We next sought to assess the influence of daptomycin driven T7SS induction on inter-enterococcal antagonism. *E. faecalis* V583 and its derivatives are more sensitive to daptomycin compared to *E. faecalis* OG1RF strains (Fig. S8A – S8C), so we applied a reduced concentration of 2.5 µg/ml daptomycin in the co-culture inhibition assay to prevent daptomycin intoxication of *E. faecalis* Δpip_{V583} bystanders. Because *E. faecalis* OG1RF T7SS gene expression is less robust in the presence of 2.5 µg/ml compared to 6.25 µg/ml daptomycin, which was used in our previous experiments (Fig. 3A and S8D), a 10:1 ratio of daptomycin treated *E. faecalis* OG1RF was required for growth inhibition of *E. faecalis* Δpip_{V583} during co-culture (Fig. 3C). Consistent with our previous results, daptomycin induced T7SS inhibition of *E. faecalis* Δpip_{V583} was contact dependent (Fig. 3D). To increase T7SS mediated contact-dependent killing of the target strain during daptomycin exposure, we performed the inhibition assay on nutrient agar plates. The sub-inhibitory concentration of daptomycin (2.5 µg/ml) used in liquid culture was toxic to the cells on agar plates (Fig. S8E), so we lowered the daptomycin concentration to 0.5 µg/ml to prevent drug toxicity in the agar-based antagonism assay. Plating T7SS producing *E. faecalis* OG1RF cells and *E. faecalis* Δpip_{V583} bystander cells at a ratio of 10:1 resulted in ~10–fold inhibition of bystander growth (Fig. 3E). Although 0.5 µg/ml of daptomycin did not dramatically increase *E. faecalis* OG1RF T7SS transcript abundances, this was sufficient to promote daptomycin mediated T7SS inhibition of bystanders on agar plates

(Fig. 3E and Fig. S8E). These data show that in addition to phages, antibiotics can be sensed by *E. faecalis* thereby inducing T7SS antagonism of non-kin bacterial cells. These data also show that the magnitude of T7SS gene expression and forcing bacteria-bacteria contact is directly related to the potency of T7SS inhibition.

The primary bile acid sodium cholate does not modulate *E. faecalis* T7SS gene expression

To gain insight into host-associated environmental cues that could trigger *E. faecalis* OG1RF T7SS, we measured T7SS transcription in the presence of a sub-inhibitory concentration of the primary bile acid sodium cholate, an abundant compound found in the mammalian intestinal tract and that is known to promote bacterial cell membrane stress [57, 58]. 4% sodium cholate, a concentration that has been shown to severely impair the growth of *E. faecalis* OG1RF cell envelop mutants, caused only a minor reduction in cell density of wild type *E. faecalis* OG1RF [59] (Fig. S9A) and it did not stimulate T7SS gene expression (Fig. S9B). Collectively, these data show that T7SS induction in *E. faecalis* occurs in response to select cell envelope stressors.

IreK and OG1RF_11099 facilitate T7SS expression in phage infected *E. faecalis* OG1RF via a non-canonical signaling pathway

Having established that both phage and daptomycin mediated membrane damage independently stimulates heightened *E. faecalis* OG1RF T7SS gene expression and antagonistic activity, we next sought to identify the genetic determinants that sense this damage and promote T7SS transcription. Two-component systems, LiaR/S and CroS/R, and the PASTA kinase family protein IreK are well-characterized modulators of enterococcal cell envelope homeostasis and antimicrobial tolerance [60-62]. Aberrant cardiolipin microdomain remodeling in the bacterial cell membrane in the absence of the LiaR response regulator results in

daptomycin hypersensitivity and virulence attenuation [63]. CroS/R signaling and subsequent modulation of gene expression govern cell wall integrity and promote resistance to cephalosporins, glycopeptides and beta—lactam antibiotics [64-66]. The *ireK* encoded transmembrane Ser/Thr kinase regulates cell wall homeostasis, antimicrobial resistance, and contributes to bacterial fitness during long-term colonization of the intestinal tract [61, 67, 68]. Recently it has been shown that direct cross-talk between IreK and the CroS/R system positively impacts enterococcal cephalosporin resistance [69].

Wild type *E. faecalis* OG1RF, an *ireK* in-frame deletion mutant [61] and transposon (Tn) insertion mutants of *liaR*, *liaS*, *croR*, and *croS* [70] all display similar growth kinetics in the absence of phage VPE25 infection (Fig.S10A). Although *croR*-Tn and *croS*-Tn exhibit reductions in the plaquing efficiency of VPE25 particles, none of these genetic elements of enterococcal cell wall homeostasis and antibiotic resistance were required for VPE25 infection (Fig.S10B). We queried the expression levels of T7SS genes in these isogenic mutants during phage VPE25 infection (MOI = 1). T7SS gene expression was not enhanced in the Δ*ireK* mutant during phage infection (Fig.4A), whereas *liaR*-Tn, *liaS*-Tn, *croR*-Tn, and *croS*-Tn produced heightened levels of T7SS transcripts similar to the wild type *E. faecalis* OG1RF compared to the uninfected controls (Fig.S11A – S11F). A sub-lethal concentration of the cephalosporin ceftriaxone did not induce T7SS gene expression (Fig. S12A), indicating that expression of T7SS genes following phage mediated membrane damage signals through a pathway that is distinct from the IreK response to cephalosporin stress. Additionally, the Δ*ireK* mutant phenocopies the Δ*essB* mutant strain in the interbacterial antagonism co-culture assay, wherein the Δ*ireK* mutant is unable to mediate phage induced T7SS dependent killing of the phage resistant *E. faecalis* Δpip_{V583} non-kin cells (Fig. 4B). T7SS antagonism is restored in *E. faecalis* Δ*ireK* by introducing the wild type gene in *trans* (Fig. 4B). Collectively, these results indicate that IreK senses phage mediated membrane damage promoting T7SS transcription independent of the CroS/R pathway.

OG1RF_11099, located immediately upstream of the T7SS cluster is predicted to encode a GntR family transcriptional regulator, thus we sought to assess the contribution of OG1RF_11099 on T7SS transcription and functionality. *E. faecalis* OG1RF carrying a transposon insertion in OG1RF_11099 is equally susceptible to phage VPE25 infection compared to wild type *E. faecalis* OG1RF (Fig. S2A) In contrast to wild type *E. faecalis* OG1RF, T7SS genes were not induced during phage predation of *E. faecalis* OG1RF_11099-Tn (Fig. 4C). We evaluated the influence of OG1RF_11099-dependent regulation on the activity of T7SS in intraspecies antagonism using our co-culture assay. Similar to *E. faecalis* Δ*essB*, the OG1RF_11099-Tn mutant displayed attenuated T7SS activity in phage infected co-cultures (Fig. 4D). T7SS dependent antagonism of *E. faecalis* OG1RF_11099-Tn could be restored following complementation (Fig. 4D). Collectively, these results indicate that *OG1RF_11099* encodes a positive regulator of *E. faecalis* T7SS important for phage mediated inhibition of bystander bacteria. Given that IreK governs downstream signaling events via phosphorylation [71], and the fact that OG1RF_11099 was not differentially expressed in response to phage infection of wild type *E. faecalis* OG1RF or *ireK* mutant strains (Fig. S12B), suggests that either post-translational modification of OG1RF_11099 or a yet unidentified protein downstream of IreK engaging with OG1RF_11099 accounts for T7SS gene expression during phage infection.

Discussion

Despite the fact that bacteria exist in complex microbial communities that socially interact [72, 73], phage predation studies have primarily been performed in monoculture [24, 74-76]. Studies report phage-mediated effects on non-target bacteria linked to interbacterial interactions and evolved phage tropism for non-cognate bacteria [77-79], whereas other studies have identified minimal changes in microbiota diversity during phage therapy [77, 80].

Our results extend previous work that observed the induction of *E. faecalis* OG1RF T7SS gene expression in response to phage infection [24]. By using an *in vitro* antibacterial

antagonism assay, we discovered that phage predation of *E. faecalis* OG1RF has an inhibitory effect on non-phage targeted bacterial species during co-culture. Our work shows that phage mediated inhibition of Gram positive bystander bacteria relies on the expression and activity of T7SS genes. This work establishes a framework to begin investigating if and how phage infection of target bacteria influences non-target bacterial populations in complex communities such as the microbiota.

Our data suggest that membrane stress associated with phage infection or sub-lethal daptomycin treatment stimulates T7SS mediated antibacterial antagonism of *E. faecalis* OG1RF (Fig. 5). Given that daptomycin is used to target vancomycin-resistant enterococcal infections, this finding provides a hypothesis for how antibiotic-resistant enterococci achieve overgrowth and dominate the microbiota following antibiotic treatment. Further investigation is required to understand how T7SS induction might contribute to enterococcal fitness in polymicrobial environments. Although exposure to a sub-inhibitory level of primary bile salt (a common molecule found in the intestine) did not elicit T7SS expression, it is possible that other stressors encountered in the intestinal tract, including lysozyme, antimicrobial proteins, and nutrient availability could influence T7SS activity in *E. faecalis*. Indeed, *E. faecalis* T7SS mutants are defective in their ability to colonize the murine reproductive tract, which like the intestine is a polymicrobial environment [36].

We discovered that transcriptional activation of the T7SS during phage infection relies on IreK (Fig. 5). Previously characterized IreK–mediated stress response pathways, including cephalosporin stress or CroS/R signaling, did not contribute to T7SS expression. We hypothesize that IreK senses diverse environmental stressors and coordinates distinct outputs in response to specific stimuli. Considering that IreK signaling is important for *E. faecalis* intestinal colonization [68], it is possible that IreK–dependent T7SS expression in response to intestinal cues modulate interbacterial interactions and enterococcal persistence in the intestine. However, the molecular mechanism by which IreK facilitates T7SS transcription remains

388 unanswered. Additionally, we currently do not know if IreK directly senses phage or daptomycin
389 mediated membrane damage or some other signal feeds into IreK to facilitate T7SS induction.
390 Additionally, we discovered that *E. faecalis* OG1RF T7SS transcription is regulated a GntR-
391 family transcriptional regulator encoded by OG1RF_11099, a gene found immediately upstream
392 of the T7SS cluster (Fig. 5). Interestingly, OG1RF_11099 is highly conserved across
393 enterococci, including *E. faecalis* V583 (Fig. 1A) and other strains that lack T7SS. The presence
394 of a conserved transcriptional regulator in the absence of its target genetic region supports the
395 idea that certain strains of enterococci have undergone genome reduction as an evolutionary
396 strategy to adapt to unique host and non-host environments. It is possible that in *E. faecalis*
397 V583, the OG1RF_11099 homolog (EF1328) has been retained to regulate other genes within
398 the regulon that are less dispensable than T7SS. Additionally, our data indicate that
399 OG1RF_11099 transcription is not dependent on IreK or and is not induced during phage
400 infection of wild type *E. faecalis* OG1RF. Previously published work demonstrated that IreK
401 kinase activity is essential for driving the cell wall stress response in *E. faecalis* [67, 71].
402 Therefore, we hypothesize that IreK directly or indirectly regulates OG1RF_11099 activity for
403 T7SS expression via post-translational modification.
404 Antibacterial properties of T7SS substrates have been demonstrated [26, 27, 40]. Here we
405 provide evidence that mutation in the LXG toxin encoded by OG1RF_11121 abrogates phage
406 induced T7SS dependent inhibition of bystander bacteria while expression of the downstream
407 immunity gene OG1RF_11122 in T7SS targeted *E. faecalis* Δpip_{V583} cells conferred partial
408 protection from this inhibition. It is possible that constitutive expression of OG1RF_11122 from a
409 multicopy plasmid results in elevated accumulation of OG1RF_11122 in the bystander strain
410 which is toxic and could account for the partial protection phenotype. Aside from its LXG
411 domain, OG1RF_11121 does not harbor any other recognizable protein domains, hence the
412 mechanism underlying its toxicity is unclear. Whitney *et al.* demonstrated that LXG toxin
413 antagonism is contact–dependent, having minimal to no impact on target cells in liquid media

414 [27]. Although we found that physical engagement is crucial for *E. faecalis* T7SS mediated
415 antagonism, we observed a significant reduction in target cell growth in liquid media both during
416 phage and daptomycin treatment of T7SS proficient *E. faecalis*.

417 In contrast to the broad antagonism of *S. intermedius* T7SS [27], the *E. faecalis* OG1RF
418 T7SS targets a more limited number of bacterial species. Interestingly, *E. faecalis* OG1RF T7SS
419 antagonism is ineffective against various species of streptococci, which like the enterococci are
420 lactic acid bacteria. Nucleotide– and protein–based homology searches did not reveal
421 homologs of candidate immunity proteins, OG1RF_11110, OG1RF_11112, OG1RF_11122, or
422 OG1RF_12413, in *S. agalactiae* COH1. Genome sequences of the other four streptococci used
423 in this present study are not available, and hence we cannot comment on the presence of
424 potential immunity proteins against OG1RF T7SS toxins in these strains. However, resistance of
425 multiple streptococcal species to OG1RF T7SS mediated inhibition suggest that common cell
426 surface modifications, e.g., capsule or surface polysaccharides, might be responsible for
427 blocking toxin activity. Narrow target range is a common attribute of contact-dependent toxins
428 that interact with specific membrane receptors on target cells to exert inhibitory activity [81].
429 However, specific receptors of T7SS toxins are yet to be identified. It is possible that specific or
430 non-specific interactions between the *E. faecalis* OG1RF and *S. aureus* or *L. monocytogenes*
431 cell surfaces facilitate T7SS interbacterial antagonism and such interactions are incompatible or
432 occluded for the streptococci.

433 It is currently unknown whether T7SS toxin delivery requires contact with a receptor on
434 target cells or whether delivery can occur in the absence of a receptor. Examples of both
435 methods of toxin delivery are widespread in bacteria. Toxins such as colicins and R-pyocins
436 mediate contact with target cells via protein receptors and LPS, respectively [82-84]. Delivery of
437 colicins and toxins produced by contact-dependent inhibition systems in Gram-negative bacteria
438 requires interactions with receptors at the outer and inner membranes [85, 86]. Conversely, the
439 T6SS needle-like machinery that punctures target cell envelopes delivers toxins in a contact-

dependent, receptor-independent manner [87]. Cell surface moieties can also affect recognition of target cells and subsequent toxin delivery. The presence of capsule can block target cell recognition by contact-dependent growth inhibition systems in *Acinetobacter baumannii* [88], *E. coli* [89] and *Klebsiella pneumoniae* [90]. Therefore, it is possible that a feature of the streptococcal cell surface, such as capsule modifications, renders them insensitive to killing by toxins delivered by the *E. faecalis* OG1RF T7SS.

Enterococci occupy polymicrobial infections often interacting with other bacteria [91-94]. Although commensal *E. faecalis* antagonize virulent *S. aureus* through the production of superoxide [95], the two species also exhibit growth synergy via exchange of critical nutrients [96]. Here, we show that phage treatment of *E. faecalis* OG1RF can indirectly impact the growth of neighboring phage-resistant bacteria, including *S. aureus*, in a T7SS–dependent manner, suggesting that phage therapy directed against enterococci driving T7SS activity could be useful for the treatment of polymicrobial infections. However, the counter argument is that phage therapy directed against enterococci could push a bacterial community toward dysbiosis, as phage induced T7SS activity could directly inhibit beneficial bystander bacteria. This raises questions about the consequences of phage mediated off-target effects on bacteria. Could phage induced T7SS activity be used to reduce phage expansion into other closely related strains as a means to dilute phages out of a population, or is it simply that phage induction of the T7SS serves as a mechanism that benefits a select few within a population to aid in their reoccupation of a niche upon overcoming phage infection? Future studies aimed at exploring enterococcal T7SS antagonism in polymicrobial communities should help elucidate the impact of phages on microbial community composition.

Materials and Methods

Bacteria and bacteriophages. Bacteria and phages used in this study are listed in Table S1. Bacteria were grown with aeration in Todd-Hewitt broth (THB) or on THB agar supplemented

with 10mM $MgSO_4$ at 37°C. The following antibiotic concentrations were added to media for the selection of specific bacterial strains or species: *E. faecalis* OG1RF (25 µg/ml fusidic acid, 50 µg/ml rifampin), *E. faecalis* V583 Δpip_{V583} (25 µg/ml or 100 µg/ml gentamicin in liquid and agar media, respectively), *S. aureus* AH2146 LAC Φ11:LL29 (1 µg/ml tetracycline), *L. monocytogenes* 10403S (100 µg/ml streptomycin), *S. gordonii* ATCC® 49818 (500 µg/ml streptomycin), *S. salivarius* K12 (100 µg/ml spectinomycin), *V. cholerae* C6706 int I4::TnFL63 and *S. enterica* serovar Typhimurium 140285 put::Kan (50 µg/ml kanamycin). *S. agalactiae* COH1 was distinguished from *E. faecalis* on Chrome indicator Agar (CHROMagar StrepB SB282). We were unable to differentially select *E. coli, L. lactis*, *S. pyogenes* and *S. mitis* from *E. faecalis* based on antibiotic sensitivity. Therefore, colony counts of these bacteria in co-culture experiments were acquired by subtracting the *E. faecalis* colony numbers on selective media from the total number of colonies on non-selective media. Strains harboring pLZ12A and its derivatives were grown in the presence of 20 µg/ml chloramphenicol and strains carrying pCIEtm and pCIEtm derivatives were selected on media containing 5 µg/ml tetracycline.

Bioinformatic analyses. Genome sequences of *E. faecalis* V583 (NC_004668.1) and OG1RF (NC_017316.1) were obtained from NCBI. Alignments were generated and visualized using EasyFig [97]. OG1RF protein domains were identified using KEGG [98] and ExPASy PROSITE [99]. Structure modeling of OG1RF_12414 was done with Phyre2 [48]. Crystal structures overlays were generated using Pymol [100]. The EsxA phylogenetic tree was constructed in MEGA version X [101] using non-redundant protein sequences obtained from NCBI BLAST [102] with OG1RF_11100 as input and was edited using the Interactive Tree Of Life browser [103]. OG1RF_11109 was used as an input for the NCBI Conserved Domain Architecture Retrieval Tool [104] to identify protein domains that co-occur with LXG domains in *Enterococcus* (NCBI:txid1350).

Antibiotic sensitivity profiles. Antibiotic susceptibility profiles for ampicillin, vancomycin, and daptomycin were determined using a broth microdilution assay. Overnight (O/N) *E. faecalis* OG1RF cultures were diluted to 5 × 10^6 CFU/ml and 100 µl was added to each well of a 96-well plate to give a final cell density of 5 × 10^5 CFU/ml. Antibiotic stocks were added to the first column of each row, mixed thoroughly, and serially diluted 2-fold across the rows. The last column was used as a no drug control. Cultures containing daptomycin were supplemented with 50 µg/ml $CaCl_2$. Bacterial growth was monitored by measuring absorbance (OD_{600}) using a Synergy H1 microplate reader set to 37°C with continuous shaking O/N. Growth curves are presented as the average of three biological replicates. A concentration of antibiotic just below the drug amount that inhibits bacterial growth was deemed sub-lethal and used to examine T7SS genes expression.

Co-culture bacterial antagonism assays. For inter- and intraspecies antagonism assays in liquid media, O/N cultures of different bacteria were diluted in THB containing 10mM $MgSO_4$ to an OD_{600} of 0.2 and mixed together in a 1:1 or 10:1 ratio. The mixed cell suspensions were either left untreated or treated with phage VPE25 (MOI 0.01) or daptomycin (2.5 µg/ml) and grown at 37°C with aeration. For pheromone induction of genes OG1RF_11121, *ireK* and OG1RF_11099 cloned into pCIEtm, 10 ng/ml cCF10 (from Mimotopes) was added at the time of phage administration. For antagonism experiments on agar plates, O/N cultures of different strains were diluted to an OD_{600} of 0.2 and mixed together in a 1:1 or 10:1 ratio. A total of 10^7 cells from mixed culture suspension was added to 5 ml THB + 0.35% agar at 55°C and were poured over the surface of a THB agar plate in the absence or presence of daptomycin (0.5 µg/ml). The plates were incubated at 37°C under static conditions for 24 hours. Cells were harvested by scraping off the top agar, resuspending in 5 ml of PBS, and the cfus were obtained by plating serially diluted cell suspension on appropriate selective agar plates. Relative viability

517 was calculated from the ratio of target strain cfu in the treated versus the untreated co-culture.
518 The assays were performed in biological triplicates.
519
520 **RNA extraction and quantitative PCR.** RNA was extracted from phage, antibiotic, or 4%
521 sodium cholate treated or untreated *E. faecalis* OG1RF cells using an RNeasy Mini Kit (Qiagen)
522 with the following published modifications [24]. cDNA was generated from 1 µg of RNA using
523 qScript cDNA SuperMix (QuantaBio) and transcript levels were analyzed by qPCR using
524 PowerUp™ SYBR Green Master Mix (Applied Biosystems). Transcript abundances were
525 normalized to 16S rRNA gene transcripts and fold–change was calculated by comparing to
526 untreated controls. All data are represented as the average of three biological replicates.
527
528 **Bacterial growth curves.** 25 ml of 10mM $MgSO_4$ supplemented THB was inoculated with O/N
529 cultures of *E. faecalis* diluted to an OD_{600} of 0.025 and distributed to a 96-well plate in 0.1 ml
530 volumes. Cultures were incubated at 37° C with aeration. OD_{600} was measured periodically for
531 18 hours in a Synergy H1 microplate reader.
532
533 **Efficiency of plating (EOP) assays.** To investigate if phage VPE25 can infect and lyse *E.*
534 *faecalis* mutants and various other bacterial species, 10^7 PFU/ml of phage was serially diluted
535 and the phage was titered on each strain using a THB agar overlay plaque assay. EOP is
536 expressed as the percentage of phage titer from each strain relative to the wild type *E. faecalis*
537 OG1RF control. Data are presented as the average of three biological replicates.
538
539 **Construction of *E. faecalis* mutants and complementation.** Isolation of *E. faecalis* genomic
540 DNA was performed using a ZymoBIOMICS™ DNA Miniprep Kit (Zymo Research). All PCR
541 used for cloning were performed with high fidelity KOD Hot Start DNA Polymerase (EMD
542 Millipore). *E. faecalis* Δ*essB* was generated by allelic replacement by cloning an in frame *essB*

543 deletion product into pLT06 using Gibson Assembly® Master Mix (New England Biolabs),
544 integrating this construct into the chromosome, and resolving the deletion mutant by
545 homologous recombination [105-107]. For ectopic expression of putative immunity proteins,
546 coding regions of OG1RF_11110, OG1RF_11112, OG1RF_11122, and OG1RF_12413 were
547 cloned downstream of the *bacA* promoter (P_{bacA}) by restriction digestion and ligation into the
548 shuttle vector pLZ12A [20]. Coding regions of *ireK* and OG1RF_11099 were cloned downstream
549 of the cCF10 responsive promoter (P_Q) by restriction digestion and ligation into pCIE and
550 pCIEtm vectors, respectively. As attempts to clone OG1RF_11121 by itself were unsuccessful,
551 we cloned the OG1RF_11121 and OG1RF_11122 open reading frames, which overlap by 13
552 base pairs, together under the P_Q promoter in pCIEtm plasmid. Primer sequences and
553 restriction enzymes used for cloning are listed in Table S1. Plasmids were introduced into
554 electrocompetent *E. faecalis* cells as previously described [20].
555
556 **Statistical analysis.** Statistical tests were performed using GraphPad – Prism version 8.2.1.
557 For qPCR and bacterial competition assays, unpaired Student's t-tests were used. *P* values are
558 indicated in the figure legends.
559
560 **Data availability.** All raw data are available upon request.
561
562 **References**
563 1. Lebreton F, Willems RJL, Gilmore MS. *Enterococcus* diversity, origins in nature, and gut
564 colonization. In: Gilmore MS, Clewell DB, Ike Y, Shankar N, editors. Enterococci: from
565 commensals to leading causes of drug resistant infection. Boston2014.

566 2. Onderdonk AB, Bartlett JG, Louie T, Sullivan-Seigler N, Gorbach SL. Microbial synergy
567 in experimental intra-abdominal abscess. Infect Immun. 1976;13(1):22-6. Epub 1976/01/01.
568 PubMed PMID: 814099; PubMed Central PMCID: PMCPMC420571.

569 3. Weiner-Lastinger LM, Abner S, Edwards JR, Kallen AJ, Karlsson M, Magill SS, et al.
570 Antimicrobial-resistant pathogens associated with adult healthcare-associated infections:
571 Summary of data reported to the National Healthcare Safety Network, 2015-2017. Infect Control
572 Hosp Epidemiol. 2020;41(1):1-18. Epub 2019/11/27. doi: 10.1017/ice.2019.296. PubMed PMID:
573 31767041.

574 4. Arias CA, Panesso D, McGrath DM, Qin X, Mojica MF, Miller C, et al. Genetic basis for
575 *in vivo* daptomycin resistance in enterococci. N Engl J Med. 2011;365(10):892-900. Epub
576 2011/09/09. doi: 10.1056/NEJMoa1011138. PubMed PMID: 21899450; PubMed Central
577 PMCID: PMCPMC3205971.

578 5. Liu Y, Wang Y, Wu C, Shen Z, Schwarz S, Du XD, et al. First report of the multidrug
579 resistance gene *cfr* in *Enterococcus faecalis* of animal origin. Antimicrob Agents Chemother.
580 2012;56(3):1650-4. Epub 2011/12/29. doi: 10.1128/AAC.06091-11. PubMed PMID: 22203597;
581 PubMed Central PMCID: PMCPMC3294887.

582 6. Patel SN, Memari N, Shahinas D, Toye B, Jamieson FB, Farrell DJ. Linezolid resistance
583 in *Enterococcus faecium* isolated in Ontario, Canada. Diagn Microbiol Infect Dis.
584 2013;77(4):350-3. Epub 2013/10/08. doi: 10.1016/j.diagmicrobio.2013.08.012. PubMed PMID:
585 24095643.

586 7. Ubeda C, Taur Y, Jenq RR, Equinda MJ, Son T, Samstein M, et al. Vancomycin-
587 resistant Enterococcus domination of intestinal microbiota is enabled by antibiotic treatment in
588 mice and precedes bloodstream invasion in humans. J Clin Invest. 2010;120(12):4332-41. Epub

589 2010/11/26. doi: 10.1172/JCI43918. PubMed PMID: 21099116; PubMed Central PMCID:
590 PMCPMC2993598.

591 8. Zirakzadeh A, Patel R. Vancomycin-resistant enterococci: colonization, infection,
592 detection, and treatment. Mayo Clin Proc. 2006;81(4):529-36. Epub 2006/04/14. doi:
593 10.4065/81.4.529. PubMed PMID: 16610573.

594 9. Taur Y, Xavier JB, Lipuma L, Ubeda C, Goldberg J, Gobourne A, et al. Intestinal
595 domination and the risk of bacteremia in patients undergoing allogeneic hematopoietic stem cell
596 transplantation. Clin Infect Dis. 2012;55(7):905-14. Epub 2012/06/22. doi: 10.1093/cid/cis580.
597 PubMed PMID: 22718773; PubMed Central PMCID: PMCPMC3657523.

598 10. Munoz-Price LS, Lolans K, Quinn JP. Emergence of resistance to daptomycin during
599 treatment of vancomycin-resistant *Enterococcus faecalis* infection. Clin Infect Dis.
600 2005;41(4):565-6. Epub 2005/07/20. doi: 10.1086/432121. PubMed PMID: 16028170.

601 11. Palmer KL, Daniel A, Hardy C, Silverman J, Gilmore MS. Genetic basis for daptomycin
602 resistance in enterococci. Antimicrob Agents Chemother. 2011;55(7):3345-56. Epub
603 2011/04/20. doi: 10.1128/AAC.00207-11. PubMed PMID: 21502617; PubMed Central PMCID:
604 PMCPMC3122436.

605 12. Jasni AS, Mullany P, Hussain H, Roberts AP. Demonstration of conjugative transposon
606 (Tn5397)-mediated horizontal gene transfer between *Clostridium difficile* and *Enterococcus*
607 *faecalis*. Antimicrob Agents Chemother. 2010;54(11):4924-6. Epub 2010/08/18. doi:
608 10.1128/AAC.00496-10. PubMed PMID: 20713671; PubMed Central PMCID:
609 PMCPMC2976158.

610 13. Palmer KL, Kos VN, Gilmore MS. Horizontal gene transfer and the genomics of
611 enterococcal antibiotic resistance. Curr Opin Microbiol. 2010;13(5):632-9. Epub 2010/09/15. doi:

612 10.1016/j.mib.2010.08.004. PubMed PMID: 20837397; PubMed Central PMCID:
613 PMCPMC2955785.

614 14. Chang S, Sievert DM, Hageman JC, Boulton ML, Tenover FC, Downes FP, et al.
615 Infection with vancomycin-resistant *Staphylococcus aureus* containing the *vanA* resistance
616 gene. N Engl J Med. 2003;348(14):1342-7. Epub 2003/04/04. doi: 10.1056/NEJMoa025025.
617 PubMed PMID: 12672861.

618 15. Kurenbach B, Bohn C, Prabhu J, Abudukerim M, Szewzyk U, Grohmann E. Intergeneric
619 transfer of the *Enterococcus faecalis* plasmid pIP501 to *Escherichia coli* and *Streptomyces*
620 *lividans* and sequence analysis of its *tra* region. Plasmid. 2003;50(1):86-93. Epub 2003/06/27.
621 PubMed PMID: 12826062.

622 16. Kortright KE, Chan BK, Koff JL, Turner PE. Phage therapy: a renewed approach to
623 combat antibiotic-resistant bacteria. Cell Host Microbe. 2019;25(2):219-32. Epub 2019/02/15.
624 doi: 10.1016/j.chom.2019.01.014. PubMed PMID: 30763536.

625 17. Cheng M, Liang J, Zhang Y, Hu L, Gong P, Cai R, et al. The bacteriophage EF-P29
626 efficiently protects against lethal vancomycin-resistant *Enterococcus faecalis* and alleviates gut
627 microbiota imbalance in a murine bacteremia model. Front Microbiol. 2017;8:837. Epub
628 2017/05/26. doi: 10.3389/fmicb.2017.00837. PubMed PMID: 28536572; PubMed Central
629 PMCID: PMCPMC5423268.

630 18. Gelman D, Beyth S, Lerer V, Adler K, Poradosu-Cohen R, Coppenhagen-Glazer S, et al.
631 Combined bacteriophages and antibiotics as an efficient therapy against VRE *Enterococcus*
632 *faecalis* in a mouse model. Res Microbiol. 2018;169(9):531-9. Epub 2018/05/20. doi:
633 10.1016/j.resmic.2018.04.008. PubMed PMID: 29777835.

19. Uchiyama J, Rashel M, Takemura I, Wakiguchi H, Matsuzaki S. *In silico* and *in vivo* evaluation of bacteriophage phiEF24C, a candidate for treatment of *Enterococcus faecalis* infections. Appl Environ Microbiol. 2008;74(13):4149-63. Epub 2008/05/06. doi: 10.1128/AEM.02371-07. PubMed PMID: 18456848; PubMed Central PMCID: PMCPMC2446516.

20. Chatterjee A, Johnson CN, Luong P, Hullahalli K, McBride SW, Schubert AM, et al. Bacteriophage resistance alters antibiotic-mediated intestinal expansion of enterococci. Infect Immun. 2019;87(6):e00085-19. Epub 2019/04/03. doi: 10.1128/IAI.00085-19. PubMed PMID: 30936157; PubMed Central PMCID: PMCPMC6529655.

21. Lin DM, Koskella B, Lin HC. Phage therapy: an alternative to antibiotics in the age of multi-drug resistance. World J Gastrointest Pharmacol Ther. 2017;8(3):162-73. Epub 2017/08/23. doi: 10.4292/wjgpt.v8.i3.162. PubMed PMID: 28828194; PubMed Central PMCID: PMCPMC5547374.

22. Loc-Carrillo C, Abedon ST. Pros and cons of phage therapy. Bacteriophage. 2011;1(2):111-4. Epub 2012/02/16. doi: 10.4161/bact.1.2.14590. PubMed PMID: 22334867; PubMed Central PMCID: PMCPMC3278648.

23. Wu S, Zachary E, Wells K, Loc-Carrillo C. Phage Therapy: future inquiries. Postdoc J. 2013;1(6):24-35. Epub 2013/06/01. PubMed PMID: 28286802; PubMed Central PMCID: PMCPMC5342839.

24. Chatterjee A, Willett JLE, Nguyen UT, Monogue B, Palmer KL, Dunny GM, et al. Parallel Genomics Uncover Novel Enterococcal-Bacteriophage Interactions. mBio. 2020;11(2). Epub 2020/03/05. doi: 10.1128/mBio.03120-19. PubMed PMID: 32127456; PubMed Central PMCID: PMCPMC7064774.

657 25. Unnikrishnan M, Constantinidou C, Palmer T, Pallen MJ. The enigmatic Esx proteins:
658 looking beyond mycobacteria. Trends Microbiol. 2017;25(3):192-204. Epub 2016/11/30. doi:
659 10.1016/j.tim.2016.11.004. PubMed PMID: 27894646.

660 26. Cao Z, Casabona MG, Kneuper H, Chalmers JD, Palmer T. The type VII secretion
661 system of *Staphylococcus aureus* secretes a nuclease toxin that targets competitor bacteria.
662 Nat Microbiol. 2016;2:16183. Epub 2016/10/11. doi: 10.1038/nmicrobiol.2016.183. PubMed
663 PMID: 27723728; PubMed Central PMCID: PMCPMC5325307.

664 27. Whitney JC, Peterson SB, Kim J, Pazos M, Verster AJ, Radey MC, et al. A broadly
665 distributed toxin family mediates contact-dependent antagonism between Gram-positive
666 bacteria. Elife. 2017;6. Epub 2017/07/12. doi: 10.7554/eLife.26938. PubMed PMID: 28696203;
667 PubMed Central PMCID: PMCPMC5555719.

668 28. Burts ML, DeDent AC, Missiakas DM. EsaC substrate for the ESAT-6 secretion pathway
669 and its role in persistent infections of *Staphylococcus aureus*. Mol Microbiol. 2008;69(3):736-46.
670 Epub 2008/06/17. doi: 10.1111/j.1365-2958.2008.06324.x. PubMed PMID: 18554323; PubMed
671 Central PMCID: PMCPMC2597432.

672 29. Ishii K, Adachi T, Yasukawa J, Suzuki Y, Hamamoto H, Sekimizu K. Induction of
673 virulence gene expression in *Staphylococcus aureus* by pulmonary surfactant. Infect Immun.
674 2014;82(4):1500-10. Epub 2014/01/24. doi: 10.1128/IAI.01635-13. PubMed PMID: 24452679;
675 PubMed Central PMCID: PMCPMC3993393.

676 30. Lopez MS, Tan IS, Yan D, Kang J, McCreary M, Modrusan Z, et al. Host-derived fatty
677 acids activate type VII secretion in *Staphylococcus aureus*. Proc Natl Acad Sci U S A.
678 2017;114(42):11223-8. Epub 2017/10/05. doi: 10.1073/pnas.1700627114. PubMed PMID:
679 28973946; PubMed Central PMCID: PMCPMC5651732.

680 31. Tchoupa AK, Watkins KE, Jones RA, Kuroki A, Alam MT, Perrier S, et al. The type VII
681 secretion system protects *Staphylococcus aureus* against antimicrobial host fatty acids. bioRxiv.
682 2020:572172. doi: 10.1101/572172.

683 32. Bourgogne A, Garsin DA, Qin X, Singh KV, Sillanpaa J, Yerrapragada S, et al. Large
684 scale variation in *Enterococcus faecalis* illustrated by the genome analysis of strain OG1RF.
685 Genome Biol. 2008;9(7):R110. Epub 2008/07/10. doi: 10.1186/gb-2008-9-7-r110. PubMed
686 PMID: 18611278; PubMed Central PMCID: PMCPMC2530867.

687 33. Paulsen IT, Banerjei L, Myers GS, Nelson KE, Seshadri R, Read TD, et al. Role of
688 mobile DNA in the evolution of vancomycin-resistant *Enterococcus faecalis*. Science.
689 2003;299(5615):2071-4. Epub 2003/03/29. doi: 10.1126/science.1080613. PubMed PMID:
690 12663927.

691 34. Reiter WD, Palm P, Yeats S. Transfer RNA genes frequently serve as integration sites
692 for prokaryotic genetic elements. Nucleic Acids Res. 1989;17(5):1907-14. doi:
693 10.1093/nar/17.5.1907. PubMed PMID: 2467253; PubMed Central PMCID: PMCPMC317532.

694 35. Lebreton F, Manson AL, Saavedra JT, Straub TJ, Earl AM, Gilmore MS. Tracing the
695 enterococci from paleozoic origins to the hospital. Cell. 2017;169(5):849-61 e13. Epub
696 2017/05/16. doi: 10.1016/j.cell.2017.04.027. PubMed PMID: 28502769; PubMed Central
697 PMCID: PMCPMC5499534.

698 36. Alhajjar N, Chatterjee A, Spencer BL, Burcham LR, Willett JLE, Dunny GM, et al.
699 Genome-wide mutagenesis identifies factors involved in *Enterococcus faecalis* vaginal
700 adherence and persistence. Infection and Immunity. 2020:IAI.00270-20. doi: 10.1128/iai.00270-
701 20.

37. Das C, Ghosh TS, Mande SS. *In silico* dissection of type VII secretion system components across bacteria: new directions towards functional characterization. J Biosci. 2016;41(1):133-43. Epub 2016/03/08. doi: 10.1007/s12038-016-9599-8. PubMed PMID: 26949095.

38. Burts ML, Williams WA, DeBord K, Missiakas DM. EsxA and EsxB are secreted by an ESAT-6-like system that is required for the pathogenesis of *Staphylococcus aureus* infections. Proc Natl Acad Sci U S A. 2005;102(4):1169-74. Epub 2005/01/20. doi: 10.1073/pnas.0405620102. PubMed PMID: 15657139; PubMed Central PMCID: PMCPMC545836.

39. Duerkop BA, Huo W, Bhardwaj P, Palmer KL, Hooper LV. Molecular Basis for Lytic Bacteriophage Resistance in Enterococci. mBio. 2016;7(4). Epub 2016/09/01. doi: 10.1128/mBio.01304-16. PubMed PMID: 27578757; PubMed Central PMCID: PMCPMC4999554.

40. Ulhuq FR, Gomes MC, Duggan GM, Guo M, Mendonca C, Buchanan G, et al. A membrane-depolarizing toxin substrate of the *Staphylococcus aureus* type VII secretion system mediates intraspecies competition. Proc Natl Acad Sci U S A. 2020. Epub 2020/08/10. doi: 10.1073/pnas.2006110117. PubMed PMID: 32769205.

41. Garcia EC. Contact-dependent interbacterial toxins deliver a message. Curr Opin Microbiol. 2018;42:40-6. Epub 2017/10/28. doi: 10.1016/j.mib.2017.09.011. PubMed PMID: 29078204; PubMed Central PMCID: PMCPMC5899628.

42. Garcia-Bayona L, Comstock LE. Bacterial antagonism in host-associated microbial communities. Science. 2018;361(6408). Epub 2018/09/22. doi: 10.1126/science.aat2456. PubMed PMID: 30237322.

725 43. Zhang D, de Souza RF, Anantharaman V, Iyer LM, Aravind L. Polymorphic toxin
726 systems: comprehensive characterization of trafficking modes, processing, mechanisms of
727 action, immunity and ecology using comparative genomics. Biol Direct. 2012;7:18. Epub
728 2012/06/27. doi: 10.1186/1745-6150-7-18. PubMed PMID: 22731697; PubMed Central PMCID:
729 PMCPMC3482391.

730 44. Klein TA, Pazos M, Surette MG, Vollmer W, Whitney JC. Molecular basis for immunity
731 protein recognition of a type VII secretion system exported antibacterial toxin. J Mol Biol.
732 2018;430(21):4344-58. Epub 2018/09/09. doi: 10.1016/j.jmb.2018.08.027. PubMed PMID:
733 30194969; PubMed Central PMCID: PMCPMC6193138.

734 45. Jamet A, Nassif X. New players in the toxin field: polymorphic toxin systems in bacteria.
735 mBio. 2015;6(3):e00285-15. Epub 2015/05/07. doi: 10.1128/mBio.00285-15. PubMed PMID:
736 25944858; PubMed Central PMCID: PMCPMC4436062.

737 46. Poole SJ, Diner EJ, Aoki SK, Braaten BA, t'Kint de Roodenbeke C, Low DA, et al.
738 Identification of functional toxin/immunity genes linked to contact-dependent growth inhibition
739 (CDI) and rearrangement hotspot (Rhs) systems. PLoS Genet. 2011;7(8):e1002217. Epub
740 2011/08/11. doi: 10.1371/journal.pgen.1002217. PubMed PMID: 21829394; PubMed Central
741 PMCID: PMCPMC3150448.

742 47. Koskiniemi S, Garza-Sánchez F, Sandegren L, Webb JS, Braaten BA, Poole SJ, et al.
743 Selection of orphan Rhs toxin expression in evolved *Salmonella enterica* serovar Typhimurium.
744 PLoS Genet. 2014;10(3):e1004255. doi: 10.1371/journal.pgen.1004255. PubMed PMID:
745 24675981; PubMed Central PMCID: PMCPMC3967940.

746 48. Kelley LA, Mezulis S, Yates CM, Wass MN, Sternberg MJ. The Phyre2 web portal for
747 protein modeling, prediction and analysis. Nat Protoc. 2015;10(6):845-58. Epub 2015/05/07. doi:

748 10.1038/nprot.2015.053. PubMed PMID: 25950237; PubMed Central PMCID:
749 PMCPMC5298202.

750 49. Wiener M, Freymann D, Ghosh P, Stroud RM. Crystal structure of colicin Ia. Nature.
751 1997;385(6615):461-4. doi: 10.1038/385461a0. PubMed PMID: 9009197.

752 50. Tang JY, Bullen NP, Ahmad S, Whitney JC. Diverse NADase effector families mediate
753 interbacterial antagonism via the type VI secretion system. J Biol Chem. 2018;293(5):1504-14.
754 Epub 2017/12/15. doi: 10.1074/jbc.RA117.000178. PubMed PMID: 29237732; PubMed Central
755 PMCID: PMCPMC5798281.

756 51. Michalska K, Quan Nhan D, Willett JLE, Stols LM, Eschenfeldt WH, Jones AM, et al.
757 Functional plasticity of antibacterial EndoU toxins. Mol Microbiol. 2018;109(4):509-27. Epub
758 2018/06/21. doi: 10.1111/mmi.14007. PubMed PMID: 29923643; PubMed Central PMCID:
759 PMCPMC6173971.

760 52. Zhang D, Iyer LM, Aravind L. A novel immunity system for bacterial nucleic acid
761 degrading toxins and its recruitment in various eukaryotic and DNA viral systems. Nucleic Acids
762 Res. 2011;39(11):4532-52. Epub 2011/02/11. doi: 10.1093/nar/gkr036. PubMed PMID:
763 21306995; PubMed Central PMCID: PMCPMC3113570.

764 53. Klein TA, Ahmad S, Whitney JC. Contact-dependent interbacterial antagonism mediated
765 by protein secretion machines. Trends Microbiol. 2020;28(5):387-400. Epub 2020/04/17. doi:
766 10.1016/j.tim.2020.01.003. PubMed PMID: 32298616.

767 54. Andersson DI, Hughes D. Microbiological effects of sublethal levels of antibiotics. Nat
768 Rev Microbiol. 2014;12(7):465-78. Epub 2014/05/28. doi: 10.1038/nrmicro3270. PubMed PMID:
769 24861036.

770 55. Bernier SP, Surette MG. Concentration-dependent activity of antibiotics in natural
771 environments. Front Microbiol. 2013;4:20. Epub 2013/02/21. doi: 10.3389/fmicb.2013.00020.
772 PubMed PMID: 23422936; PubMed Central PMCID: PMCPMC3574975.

773 56. Yim G, Wang HH, Davies J. Antibiotics as signalling molecules. Philos Trans R Soc
774 Lond B Biol Sci. 2007;362(1483):1195-200. Epub 2007/03/16. doi: 10.1098/rstb.2007.2044.
775 PubMed PMID: 17360275; PubMed Central PMCID: PMCPMC2435582.

776 57. Flahaut S, Frere J, Boutibonnes P, Auffray Y. Comparison of the bile salts and sodium
777 dodecyl sulfate stress responses in *Enterococcus faecalis*. Appl Environ Microbiol.
778 1996;62(7):2416-20. Epub 1996/07/01. doi: 10.1128/AEM.62.7.2416-2420.1996. PubMed
779 PMID: 8779581; PubMed Central PMCID: PMCPMC168024.

780 58. Ridlon JM, Kang DJ, Hylemon PB. Bile salt biotransformations by human intestinal
781 bacteria. J Lipid Res. 2006;47(2):241-59. Epub 2005/11/22. doi: 10.1194/jlr.R500013-JLR200.
782 PubMed PMID: 16299351.

783 59. Dale JL, Cagnazzo J, Phan CQ, Barnes AM, Dunny GM. Multiple roles for Enterococcus
784 faecalis glycosyltransferases in biofilm-associated antibiotic resistance, cell envelope integrity,
785 and conjugative transfer. Antimicrob Agents Chemother. 2015;59(7):4094-105. Epub
786 2015/04/29. doi: 10.1128/AAC.00344-15. PubMed PMID: 25918141; PubMed Central PMCID:
787 PMCPMC4468649.

788 60. Kellogg SL, Kristich CJ. Functional dissection of the CroRS two-component system
789 required for resistance to cell wall stressors in *Enterococcus faecalis*. J Bacteriol.
790 2016;198(8):1326-36. Epub 2016/02/18. doi: 10.1128/JB.00995-15. PubMed PMID: 26883822;
791 PubMed Central PMCID: PMCPMC4859583.

792 61. Kristich CJ, Wells CL, Dunny GM. A eukaryotic-type Ser/Thr kinase in *Enterococcus*
793 *faecalis* mediates antimicrobial resistance and intestinal persistence. Proc Natl Acad Sci U S A.
794 2007;104(9):3508-13. Epub 2007/03/16. doi: 10.1073/pnas.0608742104. PubMed PMID:
795 17360674; PubMed Central PMCID: PMCPMC1805595.

796 62. Tran TT, Panesso D, Mishra NN, Mileykovskaya E, Guan Z, Munita JM, et al.
797 Daptomycin-resistant *Enterococcus faecalis* diverts the antibiotic molecule from the division
798 septum and remodels cell membrane phospholipids. mBio. 2013;4(4). Epub 2013/07/25. doi:
799 10.1128/mBio.00281-13. PubMed PMID: 23882013; PubMed Central PMCID:
800 PMCPMC3735187.

801 63. Reyes J, Panesso D, Tran TT, Mishra NN, Cruz MR, Munita JM, et al. A *liaR* deletion
802 restores susceptibility to daptomycin and antimicrobial peptides in multidrug-resistant
803 *Enterococcus faecalis*. J Infect Dis. 2015;211(8):1317-25. Epub 2014/11/02. doi:
804 10.1093/infdis/jiu602. PubMed PMID: 25362197; PubMed Central PMCID: PMCPMC4402337.

805 64. Comenge Y, Quintiliani R, Jr., Li L, Dubost L, Brouard JP, Hugonnet JE, et al. The
806 CroRS two-component regulatory system is required for intrinsic beta-lactam resistance in
807 *Enterococcus faecalis*. J Bacteriol. 2003;185(24):7184-92. Epub 2003/12/03. doi:
808 10.1128/jb.185.24.7184-7192.2003. PubMed PMID: 14645279; PubMed Central PMCID:
809 PMCPMC296236.

810 65. Hancock L, Perego M. Two-component signal transduction in *Enterococcus faecalis*. J
811 Bacteriol. 2002;184(21):5819-25. Epub 2002/10/11. doi: 10.1128/jb.184.21.5819-5825.2002.
812 PubMed PMID: 12374813; PubMed Central PMCID: PMCPMC135378.

813 66. Hancock LE, Perego M. Systematic inactivation and phenotypic characterization of two-
814 component signal transduction systems of *Enterococcus faecalis* V583. J Bacteriol.

2004;186(23):7951-8. Epub 2004/11/18. doi: 10.1128/JB.186.23.7951-7958.2004. PubMed PMID: 15547267; PubMed Central PMCID: PMCPMC529088.

67. Kristich CJ, Little JL, Hall CL, Hoff JS. Reciprocal regulation of cephalosporin resistance in *Enterococcus faecalis*. mBio. 2011;2(6):e00199-11. Epub 2011/11/03. doi: 10.1128/mBio.00199-11. PubMed PMID: 22045988; PubMed Central PMCID: PMCPMC3202758.

68. Banla IL, Kommineni S, Hayward M, Rodrigues M, Palmer KL, Salzman NH, et al. Modulators of *Enterococcus faecalis* cell envelope integrity and antimicrobial resistance influence stable colonization of the mammalian gastrointestinal tract. Infect Immun. 2018;86(1). Epub 2017/10/19. doi: 10.1128/IAI.00381-17. PubMed PMID: 29038125; PubMed Central PMCID: PMCPMC5736811.

69. Kellogg SL, Kristich CJ. Convergence of PASTA kinase and two-component signaling in response to cell wall stress in *Enterococcus faecalis*. J Bacteriol. 2018;200(12). Epub 2018/04/11. doi: 10.1128/JB.00086-18. PubMed PMID: 29632091; PubMed Central PMCID: PMCPMC5971478.

70. Dale JL, Beckman KB, Willett JLE, Nilson JL, Palani NP, Baller JA, et al. Comprehensive functional analysis of the *Enterococcus faecalis* core genome using an ordered, sequence-defined collection of insertional mutations in strain OG1RF. mSystems. 2018;3(5). Epub 2018/09/19. doi: 10.1128/mSystems.00062-18. PubMed PMID: 30225373; PubMed Central PMCID: PMCPMC6134198.

71. Labbe BD, Kristich CJ. Growth- and stress-induced PASTA kinase phosphorylation in *Enterococcus faecalis*. J Bacteriol. 2017;199(21). Epub 2017/08/16. doi: 10.1128/JB.00363-17. PubMed PMID: 28808126; PubMed Central PMCID: PMCPMC5626955.

838 72. Madsen JS, Sorensen SJ, Burmolle M. Bacterial social interactions and the emergence
839 of community-intrinsic properties. Curr Opin Microbiol. 2018;42:104-9. Epub 2017/12/05. doi:
840 10.1016/j.mib.2017.11.018. PubMed PMID: 29197823.

841 73. Xavier JB, Foster KR. Cooperation and conflict in microbial biofilms. Proc Natl Acad Sci
842 U S A. 2007;104(3):876-81. Epub 2007/01/11. doi: 10.1073/pnas.0607651104. PubMed PMID:
843 17210916; PubMed Central PMCID: PMCPMC1783407.

844 74. Leskinen K, Blasdel BG, Lavigne R, Skurnik M. RNA-sequencing reveals the
845 progression of phage-host interactions between phiR1-37 and *Yersinia enterocolitica*. Viruses.
846 2016;8(4):111. Epub 2016/04/26. doi: 10.3390/v8040111. PubMed PMID: 27110815; PubMed
847 Central PMCID: PMCPMC4848604.

848 75. Mojardin L, Salas M. Global transcriptional analysis of virus-host interactions between
849 phage Φphi29 and *Bacillus subtilis*. J Virol. 2016;90(20):9293-304. Epub 2016/08/05. doi:
850 10.1128/JVI.01245-16. PubMed PMID: 27489274; PubMed Central PMCID: PMCPMC5044823.

851 76. Sacher JC, Flint A, Butcher J, Blasdel B, Reynolds HM, Lavigne R, et al. Transcriptomic
852 analysis of the *Campylobacter jejuni* response to T4-like phage NCTC 12673 infection. Viruses.
853 2018;10(6). Epub 2018/06/20. doi: 10.3390/v10060332. PubMed PMID: 29914170; PubMed
854 Central PMCID: PMCPMC6024767.

855 77. De Sordi L, Khanna V, Debarbieux L. The gut microbiota facilitates drifts in the genetic
856 diversity and infectivity of bacterial viruses. Cell Host Microbe. 2017;22(6):801-8 e3. Epub
857 2017/11/28. doi: 10.1016/j.chom.2017.10.010. PubMed PMID: 29174401.

858 78. Hsu BB, Gibson TE, Yeliseyev V, Liu Q, Lyon L, Bry L, et al. Dynamic modulation of the
859 gut microbiota and metabolome by bacteriophages in a mouse model. Cell Host Microbe.

2019;25(6):803-14 e5. Epub 2019/06/09. doi: 10.1016/j.chom.2019.05.001. PubMed PMID: 31175044; PubMed Central PMCID: PMCPMC6579560.

79. Reyes A, Wu M, McNulty NP, Rohwer FL, Gordon JI. Gnotobiotic mouse model of phage-bacterial host dynamics in the human gut. Proc Natl Acad Sci U S A. 2013;110(50):20236-41. Epub 2013/11/22. doi: 10.1073/pnas.1319470110. PubMed PMID: 24259713; PubMed Central PMCID: PMCPMC3864308.

80. Dissanayake U, Ukhanova M, Moye ZD, Sulakvelidze A, Mai V. Bacteriophages reduce pathogenic *Escherichia coli* counts in mice without distorting gut microbiota. Front Microbiol. 2019;10:1984. Epub 2019/09/26. doi: 10.3389/fmicb.2019.01984. PubMed PMID: 31551950; PubMed Central PMCID: PMCPMC6748168.

81. Ruhe ZC, Wallace AB, Low DA, Hayes CS. Receptor polymorphism restricts contact-dependent growth inhibition to members of the same species. mBio. 2013;4(4). Epub 2013/07/25. doi: 10.1128/mBio.00480-13. PubMed PMID: 23882017; PubMed Central PMCID: PMCPMC3735181.

82. Cascales E, Buchanan SK, Duche D, Kleanthous C, Lloubes R, Postle K, et al. Colicin biology. Microbiol Mol Biol Rev. 2007;71(1):158-229. Epub 2007/03/10. doi: 10.1128/MMBR.00036-06. PubMed PMID: 17347522; PubMed Central PMCID: PMCPMC1847374.

83. Ruhe ZC, Low DA, Hayes CS. Polymorphic toxins and their immunity proteins: diversity, evolution, and mechanisms of delivery. Annu Rev Microbiol. 2020. Epub 2020/07/19. doi: 10.1146/annurev-micro-020518-115638. PubMed PMID: 32680451.

84. Kohler T, Donner V, van Delden C. Lipopolysaccharide as shield and receptor for R-pyocin-mediated killing in *Pseudomonas aeruginosa*. J Bacteriol. 2010;192(7):1921-8. Epub

2010/02/02. doi: 10.1128/JB.01459-09. PubMed PMID: 20118263; PubMed Central PMCID: PMCPMC2838038.

85. Ruhe ZC, Nguyen JY, Xiong J, Koskiniemi S, Beck CM, Perkins BR, et al. CdiA effectors use modular receptor-binding domains to recognize target bacteria. mBio. 2017;8(2). Epub 2017/03/30. doi: 10.1128/mBio.00290-17. PubMed PMID: 28351921; PubMed Central PMCID: PMCPMC5371414.

86. Willett JL, Gucinski GC, Fatherree JP, Low DA, Hayes CS. Contact-dependent growth inhibition toxins exploit multiple independent cell-entry pathways. Proc Natl Acad Sci U S A. 2015;112(36):11341-6. Epub 2015/08/26. doi: 10.1073/pnas.1512124112. PubMed PMID: 26305955; PubMed Central PMCID: PMCPMC4568652.

87. Coulthurst S. The type VI secretion system: a versatile bacterial weapon. Microbiology. 2019;165(5):503-15. Epub 2019/03/21. doi: 10.1099/mic.0.000789. PubMed PMID: 30893029.

88. Krasauskas R, Skerniškytė J, Martinkus J, Armalytė J, Sužiedėlienė E. Capsule protects *Acinetobacter baumannii* from inter-bacterial competition mediated by CdiA toxin. Frontiers in Microbiology. 2020;11(1493). doi: 10.3389/fmicb.2020.01493.

89. Aoki SK, Malinverni JC, Jacoby K, Thomas B, Pamma R, Trinh BN, et al. Contact-dependent growth inhibition requires the essential outer membrane protein BamA (YaeT) as the receptor and the inner membrane transport protein AcrB. Mol Microbiol. 2008;70(2):323-40. Epub 2008/09/03. doi: 10.1111/j.1365-2958.2008.06404.x. PubMed PMID: 18761695; PubMed Central PMCID: PMCPMC2579741.

90. Virtanen P, Wäneskog M, Koskiniemi S. Class II contact-dependent growth inhibition (CDI) systems allow for broad-range cross-species toxin delivery within the Enterobacteriaceae

905 family. Mol Microbiol. 2019;111(4):1109-25. Epub 2019/03/18. doi: 10.1111/mmi.14214.
906 PubMed PMID: 30710431; PubMed Central PMCID: PMCPMC6850196.

907 91. Flores-Mireles AL, Walker JN, Caparon M, Hultgren SJ. Urinary tract infections:
908 epidemiology, mechanisms of infection and treatment options. Nat Rev Microbiol.
909 2015;13(5):269-84. Epub 2015/04/09. doi: 10.1038/nrmicro3432. PubMed PMID: 25853778;
910 PubMed Central PMCID: PMCPMC4457377.

911 92. Giacometti A, Cirioni O, Schimizzi AM, Del Prete MS, Barchiesi F, D'Errico MM, et al.
912 Epidemiology and microbiology of surgical wound infections. J Clin Microbiol. 2000;38(2):918-
913 22. Epub 2000/02/03. PubMed PMID: 10655417; PubMed Central PMCID: PMCPMC86247.

914 93. Keogh D, Tay WH, Ho YY, Dale JL, Chen S, Umashankar S, et al. Enterococcal
915 metabolite cues facilitate interspecies niche modulation and polymicrobial infection. Cell Host
916 Microbe. 2016;20(4):493-503. Epub 2016/10/14. doi: 10.1016/j.chom.2016.09.004. PubMed
917 PMID: 27736645; PubMed Central PMCID: PMCPMC5076562.

918 94. Goh HMS, Yong MHA, Chong KKL, Kline KA. Model systems for the study of
919 enterococcal colonization and infection. Virulence. 2017;8(8):1525-62. Epub 2017/01/20. doi:
920 10.1080/21505594.2017.1279766. PubMed PMID: 28102784; PubMed Central PMCID:
921 PMCPMC5810481.

922 95. King KC, Brockhurst MA, Vasieva O, Paterson S, Betts A, Ford SA, et al. Rapid
923 evolution of microbe-mediated protection against pathogens in a worm host. ISME J.
924 2016;10(8):1915-24. Epub 2016/03/16. doi: 10.1038/ismej.2015.259. PubMed PMID: 26978164;
925 PubMed Central PMCID: PMCPMC5029159.

926 96. Hammer ND, Cassat JE, Noto MJ, Lojek LJ, Chadha AD, Schmitz JE, et al. Inter- and
927 intraspecies metabolite exchange promotes virulence of antibiotic-resistant *Staphylococcus*

928 *aureus*. Cell Host Microbe. 2014;16(4):531-7. Epub 2014/10/10. doi:
929 10.1016/j.chom.2014.09.002. PubMed PMID: 25299336; PubMed Central PMCID:
930 PMCPMC4197139.

931 97. Sullivan MJ, Petty NK, Beatson SA. Easyfig: a genome comparison visualizer.
932 Bioinformatics. 2011;27(7):1009-10. Epub 2011/01/28. doi: 10.1093/bioinformatics/btr039.
933 PubMed PMID: 21278367; PubMed Central PMCID: PMCPMC3065679.

934 98. Kanehisa M, Goto S. KEGG: kyoto encyclopedia of genes and genomes. Nucleic Acids
935 Res. 2000;28(1):27-30. doi: 10.1093/nar/28.1.27. PubMed PMID: 10592173; PubMed Central
936 PMCID: PMCPMC102409.

937 99. Sigrist CJ, de Castro E, Cerutti L, Cuche BA, Hulo N, Bridge A, et al. New and
938 continuing developments at PROSITE. Nucleic Acids Res. 2013;41(Database issue):D344-7.
939 Epub 2012/11/17. doi: 10.1093/nar/gks1067. PubMed PMID: 23161676; PubMed Central
940 PMCID: PMCPMC3531220.

941 100. DeLano WD. The PyMOL Molecular Graphics System, 1.3. Schroedinger, LLC2010.

942 101. Kumar S, Stecher G, Li M, Knyaz C, Tamura K. MEGA X: Molecular Evolutionary
943 Genetics Analysis across computing platforms. Mol Biol Evol. 2018;35(6):1547-9. doi:
944 10.1093/molbev/msy096. PubMed PMID: 29722887; PubMed Central PMCID:
945 PMCPMC5967553.

946 102. Coordinators NR. Database resources of the National Center for Biotechnology
947 Information. Nucleic Acids Res. 2018;46(D1):D8-D13. doi: 10.1093/nar/gkx1095. PubMed
948 PMID: 29140470; PubMed Central PMCID: PMCPMC5753372.

949 103. Letunic I, Bork P. Interactive Tree Of Life (iTOL) v4: recent updates and new
950 developments. Nucleic Acids Res. 2019;47(W1):W256-W9. doi: 10.1093/nar/gkz239. PubMed
951 PMID: 30931475; PubMed Central PMCID: PMCPMC6602468.

952 104. Geer LY, Domrachev M, Lipman DJ, Bryant SH. CDART: protein homology by domain
953 architecture. Genome Res. 2002;12(10):1619-23. doi: 10.1101/gr.278202. PubMed PMID:
954 12368255; PubMed Central PMCID: PMCPMC187533.

955 105. Barnes WM. PCR amplification of up to 35-kb DNA with high fidelity and high yield from
956 lambda bacteriophage templates. Proc Natl Acad Sci U S A. 1994;91(6):2216-20. Epub
957 1994/03/15. PubMed PMID: 8134376; PubMed Central PMCID: PMCPMC43341.

958 106. Gibson DG, Young L, Chuang RY, Venter JC, Hutchison CA, 3rd, Smith HO. Enzymatic
959 assembly of DNA molecules up to several hundred kilobases. Nat Methods. 2009;6(5):343-5.
960 Epub 2009/04/14. doi: 10.1038/nmeth.1318. PubMed PMID: 19363495.

961 107. Thurlow LR, Thomas VC, Hancock LE. Capsular polysaccharide production in
962 *Enterococcus faecalis* and contribution of CpsF to capsule serospecificity. J Bacteriol.
963 2009;191(20):6203-10. Epub 2009/08/18. doi: 10.1128/JB.00592-09. PubMed PMID: 19684130;
964 PubMed Central PMCID: PMCPMC2753019.

965 108. Krogh A, Larsson B, von Heijne G, Sonnhammer EL. Predicting transmembrane protein
966 topology with a hidden Markov model: application to complete genomes. J Mol Biol.
967 2001;305(3):567-80. doi: 10.1006/jmbi.2000.4315. PubMed PMID: 11152613.

968

969 **Acknowledgments**

970 This work was supported by National Institutes of Health grants R01AI141479 (B.A.D.) and
971 R01AI122742 (G.M.D.). J.L.E.W. was supported by American Heart Association Grant

19POST34450124 / Julia Willett / 2018. We would like to thank Andrés Vázquez-Torres, Laurel Lenz, Alex Horswill, Stefan Pukatzki, Kelly Doran, and their lab members for sharing bacterial strains used in this study. We thank Michelle Korir for the *ireK* complementation plasmid construct and strain.

Author Contributions

A.C., J.L.E.W., G.M.D. and B.A.D. designed the study. A.C. and J.L.E.W. perfromed experiemtns and bioinformatic analyses. A.C., J.L.E.W., G.M.D. and B.A.D. analyzed data. A.C., J.L.E.W. and B.A.D. wrote the paper with input from G.M.D.

Corresponding author

Address coorespondence to Breck A. Duerkop breck.duerkop@cuanschutz.edu

Competing Interests

There are no competing interests to report for this work.

Figure Legends

Figure 1. Phage mediated inhibition of bystander bacteria is dependent on enterococcal T7SS. (A) Diagram showing the location of T7SS genes in *E. faecalis* OG1RF (NC_017316.1) compared to *E. faecalis* V583 (NC_004668.1). Sequences were obtained from NCBI, and homology comparisons were rendered in EasyFig. Nucleotide alignments generated by Clustal Omega are enlarged for clarity (dashed lines). Stop codons of genes EF1328/OG1RF_11099 and EF1337/OG1RF_11127 are boxed. **(B)** Schematic representation of the co-culture assay used to assess the viability of bystander bacteria during phage induced T7SS activity of wild type *E. faecalis* OG1RF and Δ*essB*. Relative viability of bystander strains is calculated by

998 measuring the ratio of bystander cfus in the phage infected culture compared to the bystander
999 cfus from an uninfected control culture. **(C)** The relative abundance of viable bystander
1000 bacterium *E. faecalis* Δ*pip*$_{V583}$. Complementation of the *E. faecalis* Δ*essB* mutant, Δ*essB*
1001 (pLZ12A::*essB*), restores T7SS dependent bystander inhibition**.** Δ*essB* (pLZ12A) is the empty
1002 vector control. **(D)** T7SS inhibition of other bacterial species in the presence and absence of
1003 phage infected *E. faecalis* OG1RF or Δ*essB*. Data represent three biological replicates. Error
1004 bars indicate standard deviation. **P* < 0.00001 by unpaired Student's t-test.
1005
1006 **Figure 2. Identification of *E. faecalis* T7SS toxin and immunity proteins that dictate**
1007 **bystander growth inhibition. (A)** Putative toxin-encoding genes in the OG1RF T7SS locus.
1008 LXG domains in OG1RF_11109 and OG1RF_11121 were identified using KEGG and ExPASy
1009 PROSITE. Putative orphan toxins were identified by homology to OG1RF_11109 or
1010 OG1RF_11121. Gray lines between diagrams indicate the regions and degree of nucleotide
1011 conservation between genes. Homology diagrams were rendered in EasyFig. Gene colors for
1012 OG1RF_11109, OG1RF_11111, and OG1RF_11121 match the color scheme in panel **(B)**.
1013 OG1RF_11113 and OG1RF_11123 are shaded black to indicate that their corresponding
1014 immunity genes were not tested in panel **(B)**. **(B)** *E. faecalis* OG1RF T7SS mediated growth
1015 inhibition of phage resistant *E. faecalis* Δ*pip*$_{V583}$ during infection is alleviated by expressing
1016 OG1RF_11122 in *E. faecalis* Δ*pip*$_{V583}$ but not in the presence of pLZ12A empty vector, or
1017 expressing OG1RF_11110, OG1RF_11112, or OG1RF_12413. **(C – D)** Disruption of
1018 OG1RF_11121 by a transposon insertion rescues growth of phage resistant *E. faecalis* Δ*pip*$_{V583}$
1019 **(C)** and *S. aureus* **(D)** strains during co-culture**.** Complementation of OG1RF_11121-Tn restores
1020 bystander intoxication. Data represent three biological replicates. Error bars indicate standard
1021 deviation. **P* < 0.0001 by unpaired Student's t-test.
1022

Figure 3. Sub-lethal antibiotic treatment enhances T7SS gene expression leading to inhibition of bystander bacteria. Altered expression of T7SS genes upon exposure to sub-inhibitory concentrations of **(A)** ampicillin (0.19 µg/ml), vancomycin (0.78 µg/ml) or daptomycin (6.25 µg/ml) and **(B)** ciprofloxacin (2 µg/ml) or mitomycin C (4 µg/ml) for 40 minutes relative to the untreated control. *clpX* is shown as a negative control. **(C-E)** Contact–dependent T7SS mediated inhibition of bystander bacteria in the presence of daptomycin. Relative viability of *E. faecalis* Δpip_{V583} was measured during co-culture with *E. faecalis* OG1RF or Δ*essB* antagonists in the presence and absence of daptomycin treatment in **(C)** liquid culture (2.5 µg/ml daptomycin), **(D)** trans-well plates to prevent physical engagement between cells (2.5 µg/ml daptomycin) and **(E)** in contact on agar media (0.5 µg/ml daptomycin). Δ*essB* (pLZ12A) and Δ*essB* (pLZ12A::*essB*) represent the empty vector control and complemented strains. Data show three biological replicates. Error bars indicate standard deviation. *$P < 0.01$, **$P < 0.001$ to 0.0001 by unpaired Student's t-test.

Figure 4. IreK and OG1RF_11099 control transcription of enterococcal T7SS genes and subsequent inhibition of bystander bacteria during phage infection. (A) Phage infection leads to enhanced expression of T7SS genes in wild type *E. faecalis* OG1RF but not in a Δ*ireK* mutant strain. **(B)** Growth inhibition of *E. faecalis* Δpip_{V583} during phage infection of *E. faecalis* OG1RF is abrogated in the Δ*essB* and Δ*ireK* mutants carrying empty pCIEtm. pCIEtm::*ireK* complemented the T7SS activity defect of the Δ*ireK* strain. **(C)** Disruption of OG1RF_11099 leads to reduced expression of T7SS genes during phage infection. The data are represented as the fold change of normalized mRNA relative to uninfected samples at the same time points. **(D)** T7SS dependent intraspecies antagonism during phage infection is alleviated in the presence of OG1RF_11099-Tn mutant carrying empty pCIEtm. pCIEtm::*11099* complemented the T7SS activity defect of the OG1RF_11099-Tn mutant strain. Data represent three biological replicates. Error bars indicate standard deviation. *$P < 0.00001$ by unpaired Student's t-test.

Figure 5. A model for inhibition of bystander bacteria by the *E. faecalis* OG1RF T7SS. Phage and select antibiotics trigger a response involving IreK that results in induction of expression of T7SS genes. Transcription of T7SS genes is regulated by the predicted GntR-family transcription factor OG1RF_11099. The predicted core components of the OG1RF T7SS machinery are putative membrane proteins EsaA (OG1RF_11101), OG1RF_11102, EssB (OG1RF_11104), and EssC1 (OG1RF_11105) as well as the putative cytoplasmic protein EsaB (OG1RF_11103). EssC2 (OG1RF_11115) lacks transmembrane domains and is thus not predicted to be membrane-anchored. Upon induction of the T7SS, OG1RF_11121 is secreted from the cell, resulting in antibacterial activity against select neighboring bacteria. Expression of OG1RF_11122 can partially block toxicity caused by OG1RF_11121. Predictions of membrane topology were obtained using TMHMM [108]. The figure was created with Biorender.com.

Figure S1. Phylogenetic tree of EsxA sequences in *enterococci*. Non-redundant sequences (n=96) were identified using NCBI BLAST with OG1RF EsxA (OG1RF_11100) as the input. The tree was constructed in MEGAX using the Maximum Likelihood method and JTT matrix-based model and is drawn to scale, with branch lengths measured in the number of substitutions per site. The tree with the highest log likelihood (-3544.39) is shown. *E. faecalis* sequences are highlighted in purple, and the GenBank identifier for EsxA from OG1RF (AEA93787.1) is shown in red font.

Figure S2. Phage VPE25 infects wild type *E. faecalis* OG1RF and T7SS mutants with similar efficacy. (A) The measurement of phage particles released from wild type *E. faecalis* OG1RF, Δ*essB*, OG1RF_11121-Tn, and OG1RF_11099-Tn mutant strains following phage VPE25 infection. **(B)** Viability of strains of the OG1RF background exhibiting differential T7SS activity in the absence and presence of phage. **(C)** Viability of T7SS susceptible strains during

intraspecies competition experiments in the absence and presence of phage. Data represent three biological replicates. Error bars indicate standard deviation. *P < 0.0001 by unpaired Student's t-test.

Figure S3. Phage induced T7SS inhibitory activity is contact dependent. Intraspecies competition experiment performed in the presence of unfiltered supernatant from phage treated and untreated *E. faecalis* wild type OG1RF or Δ*essB* added **(A)** to the top of a well separated by a 0.4 μm membrane from the bottom well containing *E. faecalis* Δpip_{V583} culture, and bacterial viability was determined after 24 hours, or **(B)** directly into *E. faecalis* Δpip_{V583} culture in microtiter plate wells (P = 0.7955 by two-way analysis of variance [ANOVA]). **(C)** Growth of Δpip_{V583} was monitored in the presence of filtered supernatant from uninfected and phage infected cultures of wild type *E. faecalis* OG1RF and Δ*essB* (P = 0.0883 by two-way analysis of variance [ANOVA]). *E. faecalis* Δpip_{V583} cultures in all of these three contact-dependent assays contained gentamicin (25 μg/ml) to prevent growth of the OG1RF background strains that may have carried over in unfiltered supernatants. Error bars indicate standard deviation.

Figure S4. Putative orphan toxins in OG1RF are found as full-length LXG-domain proteins in other bacteria. OG1RF_11111, OG1RF_11113, and OG1RF_11123 sequences were used as input for NCBI BLAST. Alignments and homology were rendered in EasyFig.

Figure S5. A distal *E. faecalis* OG1RF locus encodes an additional LXG-domain protein. **(A)** Schematic showing homology between V583 (NC_004668.1, top) and OG1RF (NC_017316.1, bottom). Sequences were obtained from NCBI, and homology comparisons were rendered in EasyFig. **(B)** Cartoon depicting the LXG domain of OG1RF_12414 (identified using KEGG and ExPASy PROSITE). **(C)** Predicted structural homology between OG1RF_12414 (lilac) and the *Pseudomonas protogens* Pf-5 Tne2/Tni2 complex (PDB 6B12).

Tne2 is shown in green, and Tni2 is shown in gray. Structural modeling was done using PHYRE2, and images were rendered in Pymol.

Figure S6. Domain architecture of enterococcal LXG proteins. Domain architectures were identified using the NCBI Conserved Domain Architectural Retrieval Tool (DART) with OG1RF_11109 as an input. Diagrams are drawn to scale.

Figure S7. Antibiotic susceptibility of *E. faecalis* OG1RF. Growth of wild type *E. faecalis* OG1RF was monitored over 20 hours in the presence or absence of **(A)** ampicillin, **(B)** vancomycin and **(C)** daptomycin in microtiter plates. The antibiotic concentrations highlighted with a blue box were deemed sub-inhibitory and used to investigate T7SS gene expression levels. Early log-phase cultures of *E. faecalis* OG1RF were grown in the presence or absence of **(D)** mitomycin C (4 µg/ml) or **(E)** ciprofloxacin (2 µg/ml) to show that these concentrations of DNA targeting antibiotics do not prevent bacterial growth. Error bars indicate standard deviation.

Figure S8. Impact of daptomycin concentration on *E. faecalis* growth and T7SS induction. Growth of different enterococcal strains either untreated or treated with 6.25 µg/ml, 2.5 µg/ml or 0.5 µg/ml of daptomycin in **(A – C)** liquid media. **(D)** T7SS transcripts were measured from *E. faecalis* OG1RF cells grown in liquid media containing either no daptomycin or 6.25 µg/ml, 2.5 µg/ml, or 0.5 µg/ml of daptomycin. The data are expressed as the average of three biological replicates ± the standard deviation. $P < 0.001$ by unpaired Student's t-test. **(E)** Viable bacterial cells recovered from growth on daptomycin supplemented agar media for 24 hours. The dashed line indicates the limit of detection.

Figure S9. Effect of sub-lethal bile salt treatment on growth and T7SS transcription in *E. faecalis* OG1RF. (A) Optical density of wild type *E. faecalis* OG1RF grown in the absence and

presence of 4% sodium cholate was measured for 18 hours. **(B)** Transcript levels of OG1RF T7SS genes in untreated and 4% sodium cholate treated E. faecalis OG1RF after 4 hours. *P* < 0.001 to by unpaired Student's t-test. Error bars indicate standard deviation.

Figure S10. *E. faecalis* mutants of cell wall homeostasis show no growth defects and respond to phage VPE25 infection. (A) Optical density of wild type *E. faecalis* OG1RF and isogenic mutants were monitored for 18 hours. **(B)** While all strains were susceptible to phage VPE25 infection, the proportion of released phage particles was diminished in the *croR* and *croS* transposon mutant background. Data represent three biological replicates. Error bars indicate standard deviation. **P* < 0.001 by unpaired Student's t-test.

Figure S11. Quantitative PCR demonstrates that LiaR/S and CroS/R two-component systems do not influence T7SS gene expression during phage infection. (A- F) mRNA transcript levels of T7SS genes are enhanced in the transposon mutants of *liaR*, *liaS*, *croR* and *croS* strains similar to wild type *E. faecalis* OG1RF during phage infection (MOI = 1) compared to untreated controls. Data represent three biological replicates. Error bars indicate standard deviation. **P* < 0.01, ***P* < 0.0001 by unpaired Student's t-test.

Figure S12. Influence of sub-lethal ceftriaxone challenge and phage infection on the expression of *E. faecalis* T7SS genes. (A) Transcription of T7SS genes in *E. faecalis* OG1RF are not elevated 20 minutes post ceftriaxone (128µg/ml) administration relative to an untreated control. **(B)** OG1RF_11099 expression remains unaltered during phage predation of wild type *E. faecalis* OG1RF and Δ*ireK* strains relative to uninfected controls. Data represent three biological replicates. Error bars indicate standard deviation.

Table S1. List of bacterial strains, phages, plasmids and primers used in this study.

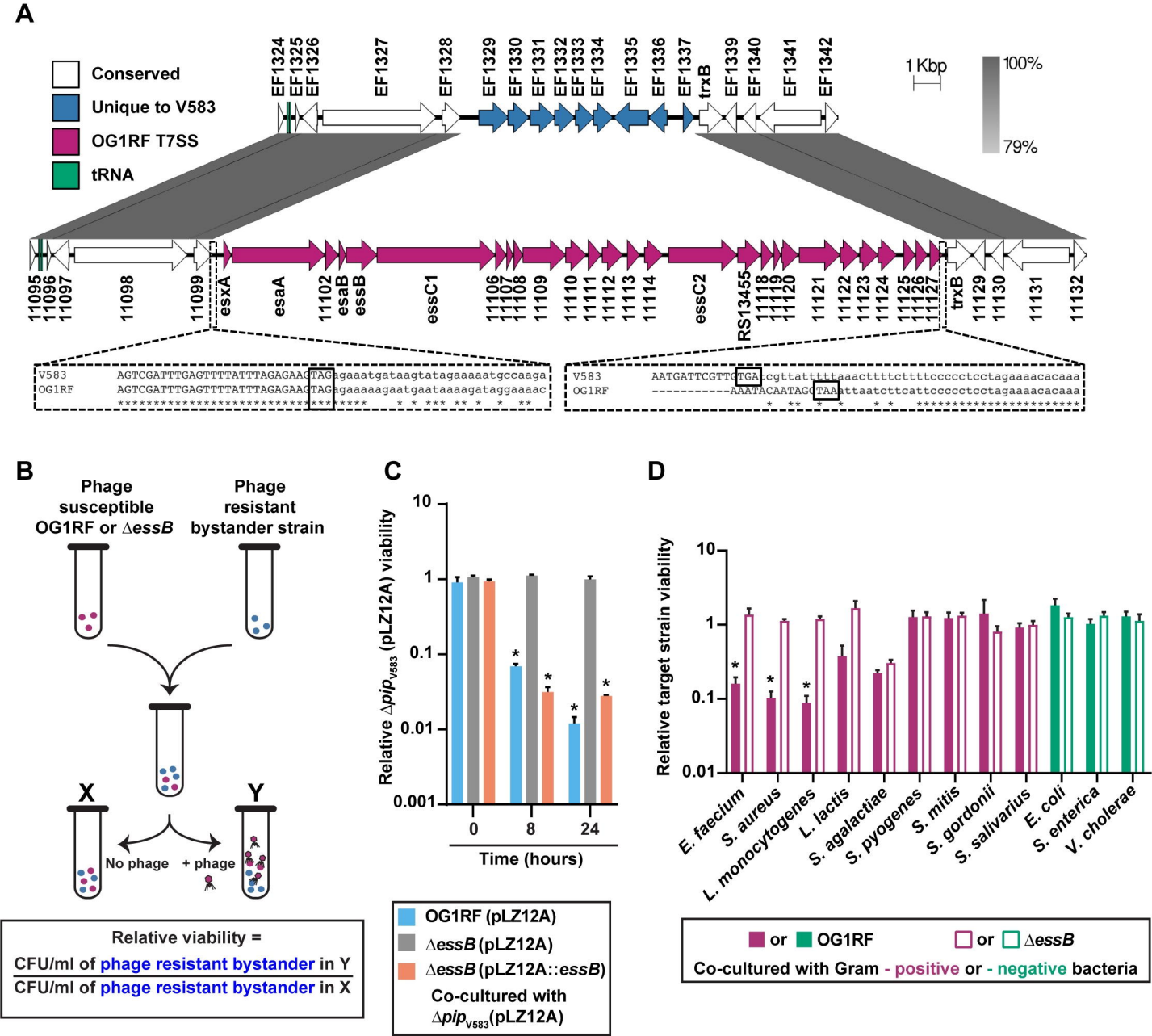
A
Conserved
Unique to V583
OG1RF T7SS
tRNA
EF1324 EF1325 EF1326 EF1327 EF1328 EF1329 EF1330 EF1331 EF1332 EF1333 EF1334 EF1335 EF1336 EF1337 trxB EF1339 EF1340 EF1341 EF1342
1 Kbp
100%
79%
11095 11096 11097 11098 11099 esxA esaA 11102 esaB essB essC1 11106 11107 11108 11109 11110 11111 11112 11113 11114 essC2 RS13455 11118 11119 11120 11121 11122 11123 11124 11125 11126 11127 trxB 11129 11130 11131 11132
V583 AGTCGATTTGAGTTTTATTTAGAGAAGTAGagaaatgataagtatagaaaaatgccaaga
OG1RF AGTCGATTTGAGTTTTATTTAGAGAAGTAGagaaaaagaatgaataaaagataggaaaac
V583 AATGATTCGTTGTGA cgttatttttaaacttttcttttccccctcctagaaaacacaaa
OG1RF ----------AAATACAATAGGTAAattaatcttcattccccctcctagaaaacacaaa
B
Phage susceptible OG1RF or ΔessB
Phage resistant bystander strain
X
Y
No phage
+ phage
Relative viability =
CFU/ml of phage resistant bystander in Y
CFU/ml of phage resistant bystander in X
C
Relative Δpip$_{V583}$ (pLZ12A) viability
10
1
0.1
0.01
0.001
0
8
24
Time (hours)
OG1RF (pLZ12A)
ΔessB (pLZ12A)
ΔessB (pLZ12A::essB)
Co-cultured with Δpip$_{V583}$(pLZ12A)
D
Relative target strain viability
10
1
0.1
0.01
E. faecium
S. aureus
L. monocytogenes
L. lactis
S. agalactiae
S. pyogenes
S. mitis
S. gordonii
S. salivarius
E. coli
S. enterica
V. cholerae
or OG1RF
or ΔessB
Co-cultured with Gram - positive or - negative bacteria

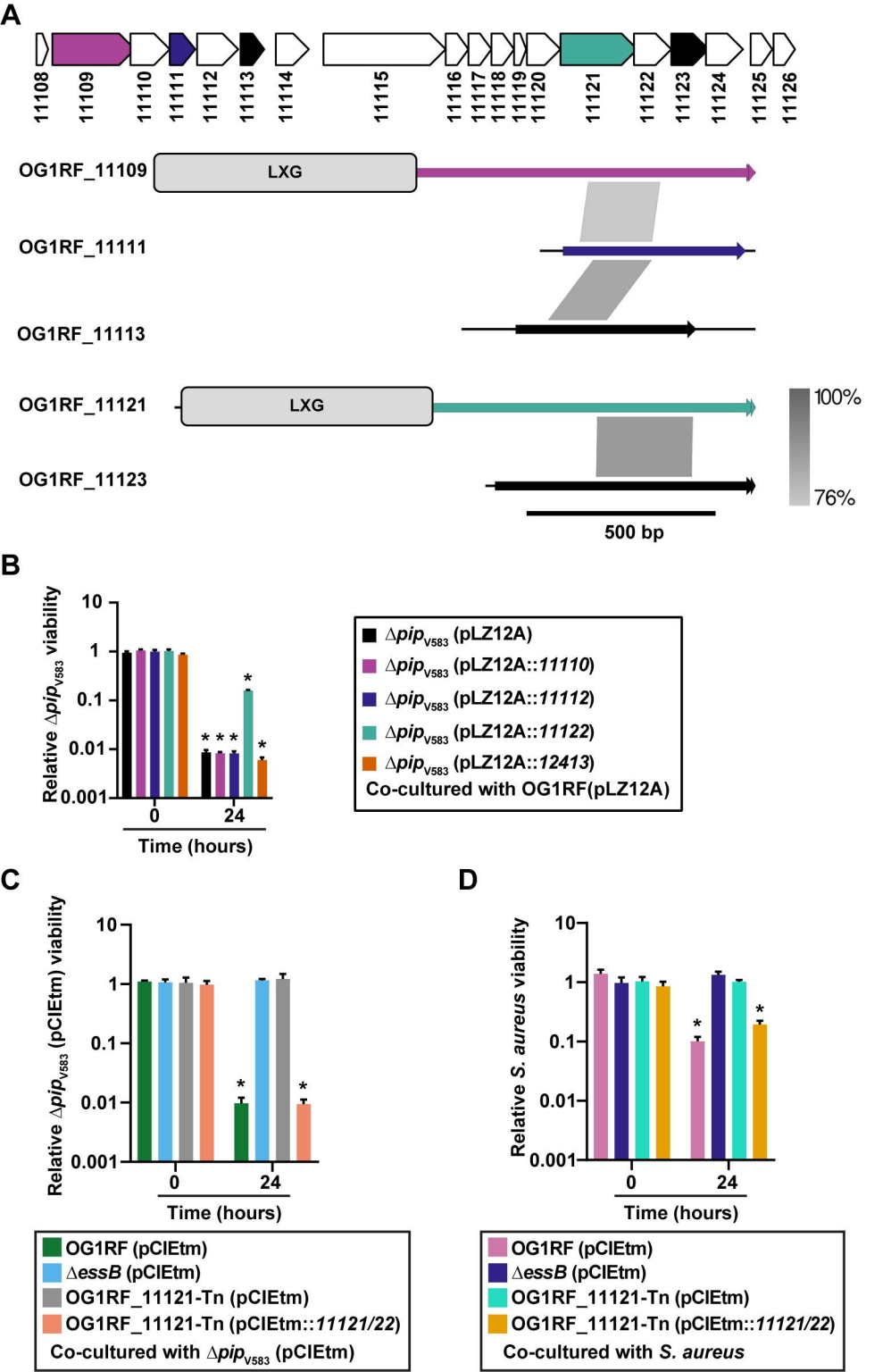
A
11108
11109
11110
11111
11112
11113
11114
11115
11116
11117
11118
11119
11120
11121
11122
11123
11124
11125
11126
OG1RF_11109
LXG
OG1RF_11111
OG1RF_11113
OG1RF_11121
LXG
OG1RF_11123
100%
76%
500 bp
B
Relative Δpip$_{V583}$ viability
10
1
0.1
0.01
0.001
0
24
Time (hours)
Δpip$_{V583}$ (pLZ12A)
Δpip$_{V583}$ (pLZ12A::11110)
Δpip$_{V583}$ (pLZ12A::11112)
Δpip$_{V583}$ (pLZ12A::11122)
Δpip$_{V583}$ (pLZ12A::12413)
Co-cultured with OG1RF(pLZ12A)
C
Relative Δpip$_{V583}$ (pCIEtm) viability
10
1
0.1
0.01
0.001
0
24
Time (hours)
OG1RF (pCIEtm)
ΔessB (pCIEtm)
OG1RF_11121-Tn (pCIEtm)
OG1RF_11121-Tn (pCIEtm::11121/22)
Co-cultured with Δpip$_{V583}$ (pCIEtm)
D
Relative S. aureus viability
10
1
0.1
0.01
0.001
0
24
Time (hours)
OG1RF (pCIEtm)
ΔessB (pCIEtm)
OG1RF_11121-Tn (pCIEtm)
OG1RF_11121-Tn (pCIEtm::11121/22)
Co-cultured with S. aureus

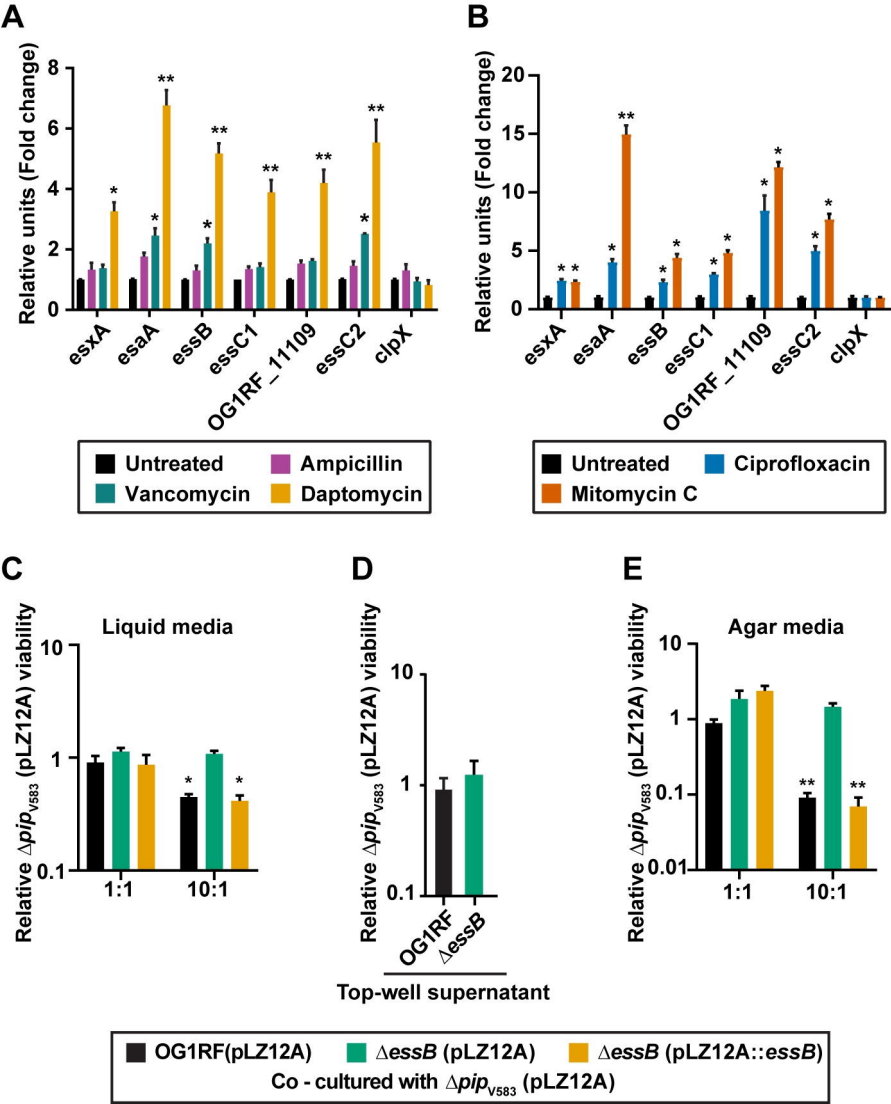
A
Relative units (Fold change)
esxA
esaA
essB
essC1
OG1RF_11109
essC2
clpX
Untreated
Ampicillin
Vancomycin
Daptomycin
B
Relative units (Fold change)
esxA
esaA
essB
essC1
OG1RF_11109
essC2
clpX
Untreated
Ciprofloxacin
Mitomycin C
C
Liquid media
Relative Δpip$_{V583}$ (pLZ12A) viability
1:1
10:1
D
Relative Δpip$_{V583}$ (pLZ12A) viability
OG1RF
ΔessB
Top-well supernatant
E
Agar media
Relative Δpip$_{V583}$ (pLZ12A) viability
1:1
10:1
OG1RF(pLZ12A)
ΔessB (pLZ12A)
ΔessB (pLZ12A::essB)
Co - cultured with Δpip$_{V583}$ (pLZ12A)

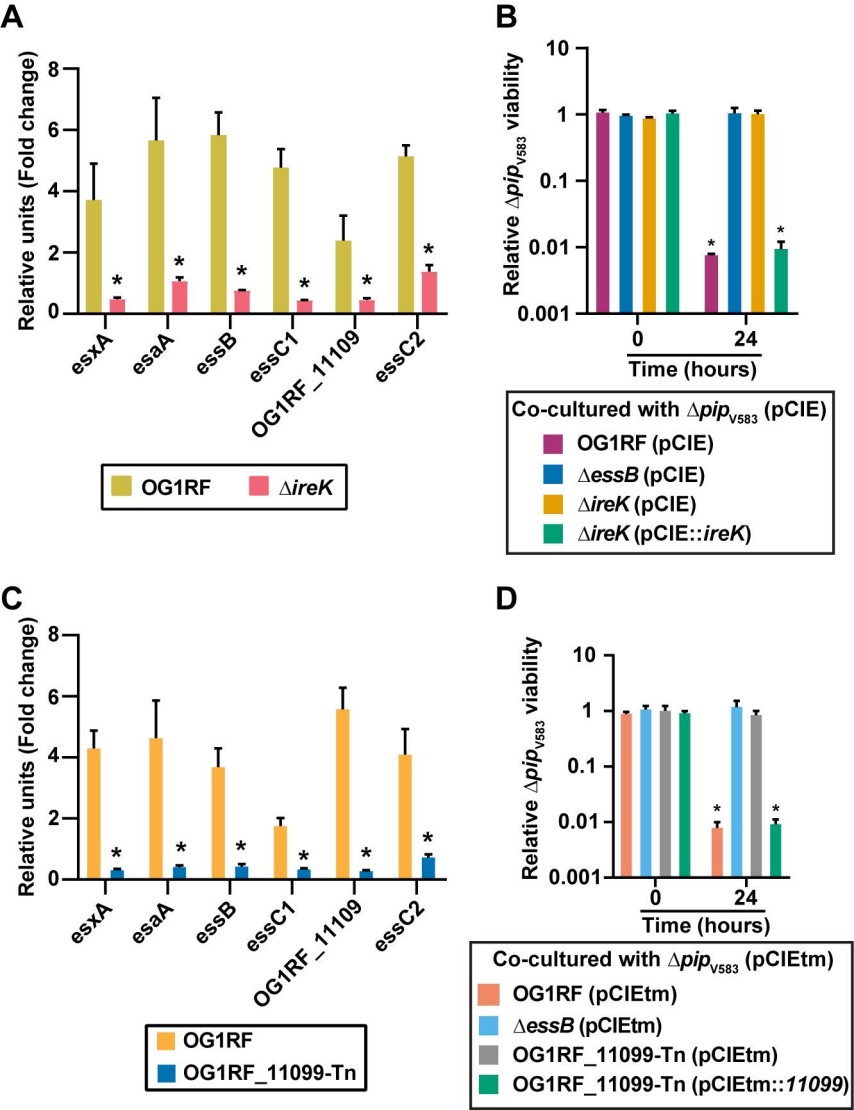
A
Relative units (Fold change)
8
6
4
2
0
esxA
esaA
essB
essC1
OG1RF_11109
essC2
OG1RF
ΔireK
B
Relative Δpip V583 viability
10
1
0.1
0.01
0.001
0
24
Time (hours)
Co-cultured with Δpip V583 (pCIE)
OG1RF (pCIE)
ΔessB (pCIE)
ΔireK (pCIE)
ΔireK (pCIE::ireK)
C
Relative units (Fold change)
8
6
4
2
0
esxA
esaA
essB
essC1
OG1RF_11109
essC2
OG1RF
OG1RF_11099-Tn
D
Relative Δpip V583 viability
10
1
0.1
0.01
0.001
0
24
Time (hours)
Co-cultured with Δpip V583 (pCIEtm)
OG1RF (pCIEtm)
ΔessB (pCIEtm)
OG1RF_11099-Tn (pCIEtm)
OG1RF_11099-Tn (pCIEtm::11099)

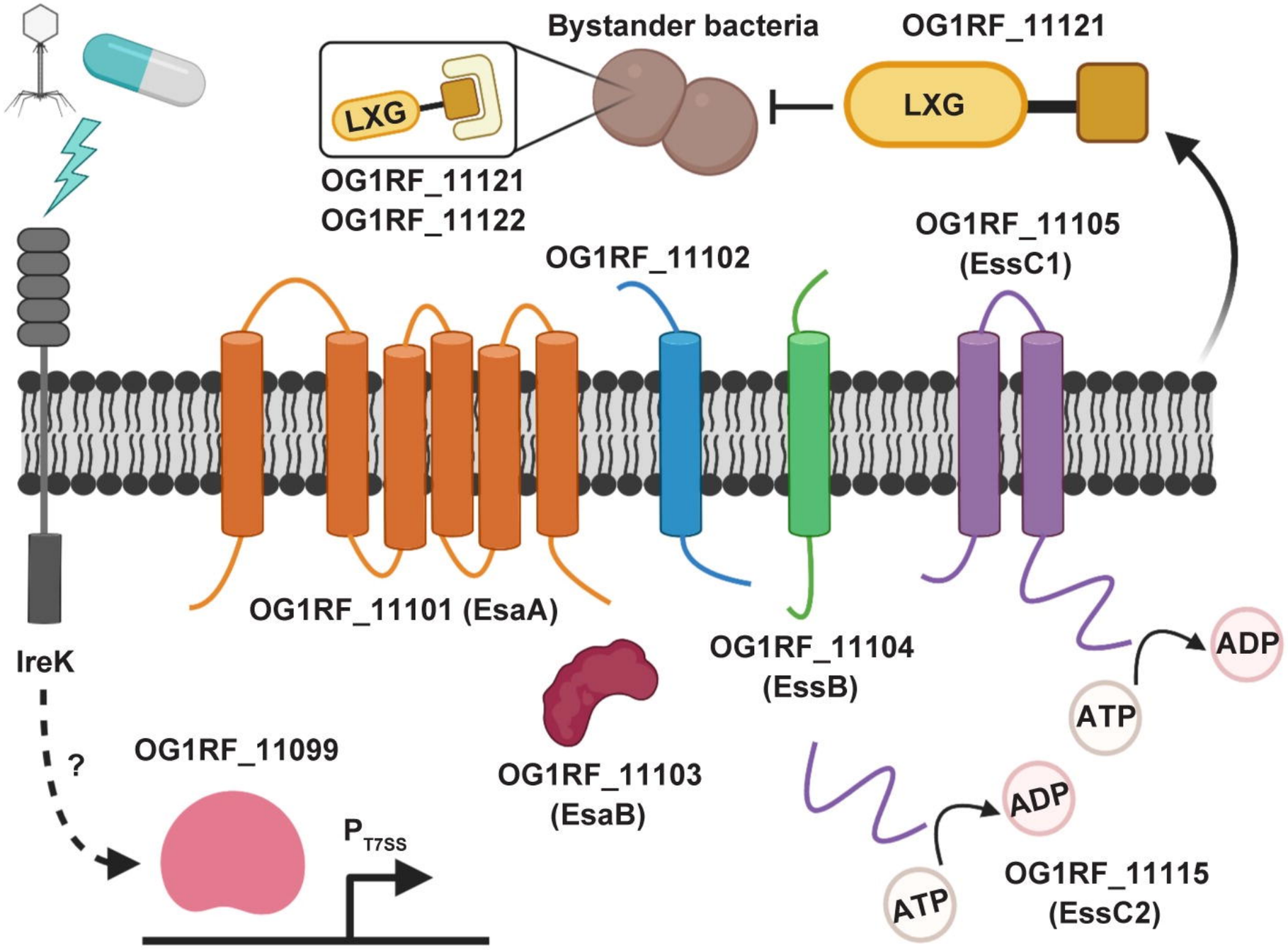
Bystander bacteria
OG1RF_11121
LXG
LXG
OG1RF_11121
OG1RF_11122
OG1RF_11105
(EssC1)
OG1RF_11102
OG1RF_11101 (EsaA)
OG1RF_11104
(EssB)
IreK
?
OG1RF_11099
OG1RF_11103
(EsaB)
P T7SS
ADP
ATP
ADP
ATP
OG1RF_11115
(EssC2)